LATERAL BRACING FORCES IN COMPRESSED TWO-SPAN COLUMNS WITH INITIAL CURVATURE

by

Jae-Guen Yang

Thesis submitted to the Graduate Faculty of the

Virginia Polytechnic Institute and State University

in partial fulfillment of the requirements for the degree of

MASTER OF SCIENCE

in

Civil Engineering

Approved:

Raymond H Plaut

R. H. Plaut, Chairman

Thomas M. Murray

T. M. Murray

W Samuel Easterling

W. S. Easterling

December, 1991

Blacksburg, Virginia

ACKNOWLEDGEMENTS

The author would like to express his deepest gratitude and appreciation to Dr. R. H. Plaut for his patient guidance and encouragement in the preparation of this thesis. Thanks also go to Dr. T. M. Murray and Dr. W. S. Easterling for their review of this thesis and comments for its improvement.

The author is also thankful to Taejin Ahn for his support.

Special thanks go to my wife, Wonkyung. Without her support and encouragement, this work would not have been possible.

Finally, very special thanks go to my parents, Mr. Seungdoo Yang and Mrs. Miza Heo Yang. Their encouragement, support, love, and faith made it possible for me to finish this thesis.

TABLE OF CONTENTS

LIST OF FIGURES

LIST OF FIGURES (cont.)

LIST OF TABLES

CHAPTER 1

INTRODUCTION

In practical design, there are various ways to increase the buckling strength of structural members. Lateral bracing is one way to increase the buckling loads of structural members, that is, to increase the load carrying capacity of the structural members. Lateral bracing for the structural members is the most effective when it has both strength and stiffness. In addition, the location of the lateral bracing plays an important role in load carrying capacity.

Under certain conditions, lateral bracing can have the same effect as an immovable lateral support. The lateral bracing is then called full bracing. If full bracing is provided, the buckling mode shape of the column is a sine curve. Point bracing for various types of columns is considered in this study.

The basic work on this subject has been done by Winter[1]. Winter investigated noncontinuous and continuous lateral bracing for both columns and beams. In order to find full bracing requirements for noncontinuous lateral supports, Winter developed a simple elementary method using fictitious hinges at the lateral supports. By taking moments about these fictitious hinges, the required stiffnesses and strengths of the supports were obtained. The bracing characteristics for cases of continuous lateral support were also determined by Winter. From Winter's investigation, the relation between the number of equal spans and the ideal spring stiffness for full bracing was obtained.

Galambos[2], Salmon and Johnson[3], and McGuire[4] outlined the work on the noncontinuous lateral bracing requirements of columns done by Winter.

Zuk[5] investigated eight typical cases of columns and beams in order to determine a general relation between the applied force or moment and the lateral bracing force. In all cases, the columns under consideration had initial imperfections. The analysis was limited to elastic materials and small deflections. It was found that the lateral force was a direct function of the initial deflection. From Zuk's investigation, it was also shown that the value of the bracing force could generally be assumed to be 2% of the applied load for axially compressed columns, and 2% of the compression flange force for beams.

Medland[6] and Medland and Segedin[7] investigated braced multiple columns and beams. The investigation was carried out to find critical loads and lateral bracing requirements for sets of interbraced columns under uniform axial force distribution and parabolic axial force distribution, respectively. In all cases, the columns were pinned at each end. Non-dimensional design charts were presented by assembling the results of a stiffness matrix solution method of initially deformed structures. The estimation of the critical loads and the strength requirements of the braces were obtained by using these design charts. It was found that the brace force was a direct function of the initial deflection.

Beliveau and Zhang[8] investigated sixteen examples of simple structures to calculate the minimum lateral stiffness by an approximate method. The critical load of a given structure was considered to be equal to the buckling load of the primary compressive member in this study. By using an approximate formulation for the change in the potential energy of the structural member, the minimum lateral stiffness was obtained. It was found that the minimum required stiffness for overall and local buckling to have the same critical load was lower when the column was fully restrained at the top node and was continuous with springs attached to a common ground than in the other examples.

The main purpose of this study is to find critical loads and full bracing conditions for perfect two-span columns, and to find the reaction forces at the lateral bracing supports and maximum deflections for two-span columns with initial curvature. The lengths of the two spans are not assumed to be equal, as they were in the references described in this section.

CHAPTER 2

ANALYSIS AND RESULTS

2.1 Perfect Columns

Several types of columns used in the analysis are shown in Figure 2.1. In each case, the column under consideration may have different bending stiffnesses EI_i, $(i=1,2)$, in each span, and the column is subjected to an axial compressive load P. As shown in Figure 2.1 (b), the simply supported column having an intermediate translational spring with stiffness $\bar{k}$ will be analyzed in Case II. The two-span column shown in Figure 2.1 (c) will be analyzed in Case III. In this case, the column has an intermediate translational spring $\bar{k}_1$ at $\bar{x}=\bar{a}$, and a lateral bracing support $\bar{k}_2$ at $\bar{x}=\bar{a}+\bar{b}=L$. For Case IV, the two-span column shown in Figure 2.1(d) will be analyzed. In this case, the column has a rotational spring $\bar{c}$ at $\bar{x}=0$, an intermediate spring $\bar{k}_1$ at $\bar{x}=\bar{a}$, and a lateral bracing support $\bar{k}_2$ at $\bar{x}=L$.

One purpose of this investigation is to find the critical load P_{cr} as a function of the span lengths. In Case II and Case III, the translational spring stiffnesses $\bar{k}_1$ and $\bar{k}_2$ will be fixed at certain values in order to show the relation between P_{cr} and $\bar{a}$. In Case IV, the rotational spring stiffness $\bar{c}$ and the two translational spring stiffnesses $\bar{k}_1$ and $\bar{k}_2$ will be fixed at certain values to show this relation.

Another purpose of this investigation is to show the effects of the rotational spring stiffness $\bar{c}$ or the translational spring stiffnesses $\bar{k}_1$ and $\bar{k}_2$ on the critical load P_{cr} for different span lengths $\bar{a}$ and $\bar{b}$. Conditions for the existence of an ideal spring stiffness are also examined. (When an ideal spring stiffness exists, higher stiffnesses do not increase the critical load.)

The transverse deflection is denoted $\bar{w}_1(\bar{x})$ for $0\le\bar{x}\le\bar{a}$ and $\bar{w}_2(\bar{x})$ for $\bar{a}\le\bar{x}\le L$. The

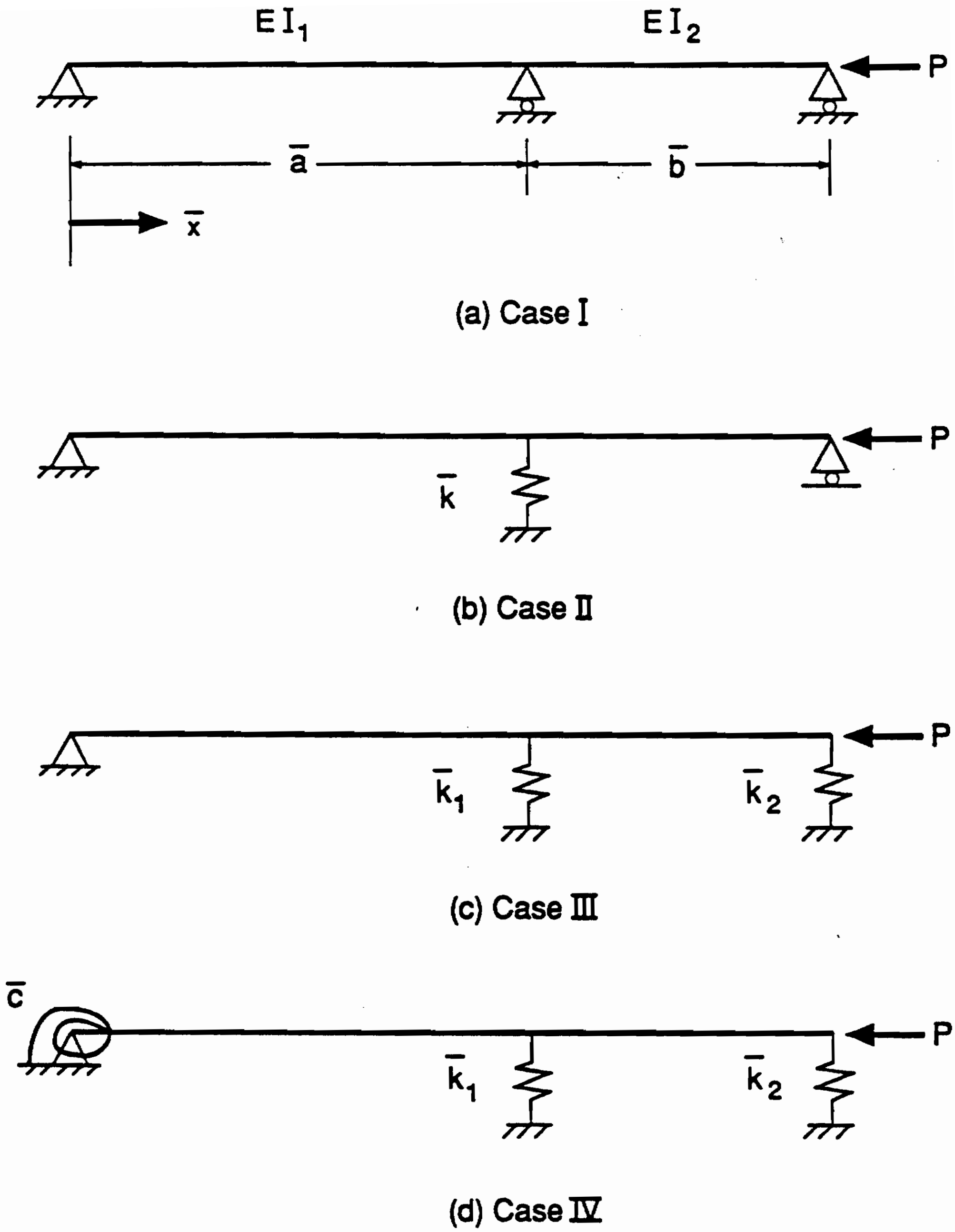

Figure 2.1 Types of Columns Used in the Analysis

equilibrium equations for each case are

$$EI_1\bar{w}_1^{////}(\bar{x})+P\bar{w}_1^{//}(\bar{x})=0,\ (0\le\bar{x}\le\bar{a})$$

and (2.1.1)

$$EI_2\bar{w}_2^{////}(\bar{x})+P\bar{w}_2^{//}(\bar{x})=0,\ (\bar{a}\le\bar{x}\le L)$$

For simplicity, nondimensional quantities are defined as follows:

$$x=\frac{\bar{x}}{L},\ a=\frac{\bar{a}}{L}$$

$$b=1-a$$

$$w_1=\frac{\bar{w}_1}{L},\ w_2=\frac{\bar{w}_2}{L} \qquad (2.1.2)$$

$$\gamma_1=\sqrt{\frac{PL^2}{EI_1}},\ \gamma_2=\sqrt{\frac{PL^2}{EI_2}}$$

$$k_1=\frac{\bar{k}_1L^3}{EI_1},\ k_2=\frac{\bar{k}_2L^3}{EI_1}$$

$$k=\frac{\bar{k}L^3}{EI_1},\ c=\frac{\bar{c}L}{EI_1}$$

$$p=\frac{PL^2}{EI_1}$$

Then the equilibrium equations and the general solutions for each case can be written as

$$w_1^{////}(x)+\gamma_1^2 w_1^{//}(x)=0$$

$$w_1(x)=A_1\sin\gamma_1 x+A_2\cos\gamma_1 x+A_3 x+A_4,\ (0\le x\le a) \qquad (2.1.3)$$

and

$$w_2^{////}(x)+\gamma_2^2 w_2^{//}(x)=0$$

$$w_2(x)=B_1\sin\gamma_2 x+B_2\cos\gamma_2 x+B_3 x+B_4,\ (a\le x\le 1) \qquad (2.1.4)$$

By applying the boundary conditions at x=0 and x=1 and the transition conditions at x=*a*, eight homogeneous algebraic equations in the eight coefficients are obtained. For buckling, the determinant of the coefficient matrix is set equal to zero. This gives the characteristic equation. Its lowest root gives the critical load.

The fundamental method that is used to compute the critical load P_{cr} and the ideal spring stiffness k_{ideal} from the characteristic equation is the bisection method. The basic concept of this method is to locate an interval where a function changes sign. If a function f(x) is real and continuous in an interval (x_l, x_u) and the function has opposite signs at x_l and x_u, so that

$$f(x_l)\,f(x_u)<0$$

then there is at least one real root within this interval. In order to find such an interval initially, the graphical method is used before the bisection method.

In all the numerical results to be presented, the column is assumed to be uniform

($EI_1=EI_2$, $\gamma_1=\gamma_2\equiv\gamma$) and the spring constants k_1 and k_2 in Case III and Case IV are assumed to be equal ($k_1=k_2\equiv k$).

a. <u>Case I: Simply Supported Two-Span Column</u>

The boundary and transition conditions for Case I are

$$w_1(0)=0, w_1''(0)=0$$

$$w_1(a)=0, w_2(a)=0$$

$$w_1'(a)=w_2'(a), \gamma_2^2 w_1''(a)=\gamma_1^2 w_2''(a) \tag{2.1.5}$$

$$w_2(1)=0, w_2''(1)=0$$

At x=*a*, the deflection is zero, and the slope and bending moment are continuous.

The characteristic equation for the buckling loads is given as follows:

$$\begin{aligned} &f_1(\gamma_1,\gamma_2,a) \\ &\equiv\gamma_2 ab\ \cos\gamma_2 b\ \sin\gamma_1 a+\gamma_1 ab\ \cos\gamma_1 a\ \sin\gamma_2 b \\ &-\sin\gamma_1 a\ \sin\gamma_2 b=0 \end{aligned} \tag{2.1.6}$$

where b=1-*a*.

If $\gamma_1=\gamma_2\equiv\gamma$, the above characteristic equation can be rewritten

$$f_2(\gamma,a)\equiv\gamma ab\ \sin\gamma-\sin\gamma a\ \sin\gamma b=0 \tag{2.1.7}$$

where $p=\gamma^2$.

The formulas of all the coefficients in terms of A_1 that are used to get the modes are as follows:

$$A_2 = 0$$

$$A_3 = -\frac{\sin\gamma_1 a}{a} A_1$$

$$A_4 = 0$$

$$B_1 = -\frac{\sin\gamma_1 a \ \cos\gamma_2}{\sin\gamma_2 b} A_1 \tag{2.1.8}$$

$$B_2 = \frac{\sin\gamma_1 a \ \sin\gamma_2}{\sin\gamma_2 b} A_1$$

$$B_3 = \frac{\sin\gamma_1 a}{b} A_1$$

$$B_4 = -\frac{\sin\gamma_1 a}{b} A_1$$

Figure 2.2 shows the critical load p_{cr} as a function of *a* when $\gamma_1=\gamma_2\equiv\gamma$. In this case, the simplified characteristic equation $f_2(\gamma,a)=0$ was used. The curves are symmetric about $a=0.5$. The critical load is $p_{cr}=4\pi^2$ (39.48) when $a=0.5$, and $p_{cr} \to 20.19$ as $a \to 0$ or $a \to 1$ (corresponding to a fixed-pinned column, since the two adjacent supports at an end cause the slope to be zero). Values of p_{cr} for different *a*'s are given in Table 1.1.

The buckling mode shapes are presented in Figure 2.3. At $a=0.5$, the buckling mode shape is a sine curve. The modes for $a>0.5$ can be obtained by symmetry. Table 1.2 shows the values of w_{1m} and w_{2m} for different *a*'s.

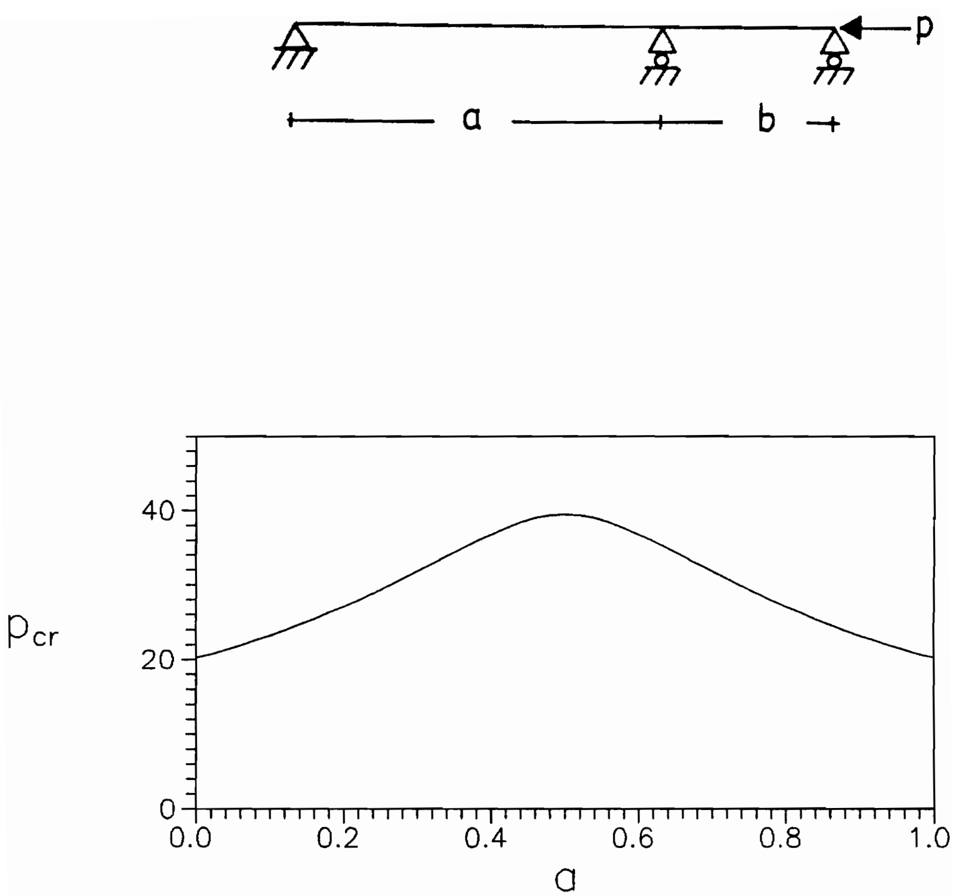

Figure 2.2 p_{cr} **for Different** ***a*****'s**

Table 1.1

p_{cr} for Different *a*'s

a	0.1	0.2	0.3	0.4	0.5
p_{cr}	23.225	27.053	31.755	36.780	39.478

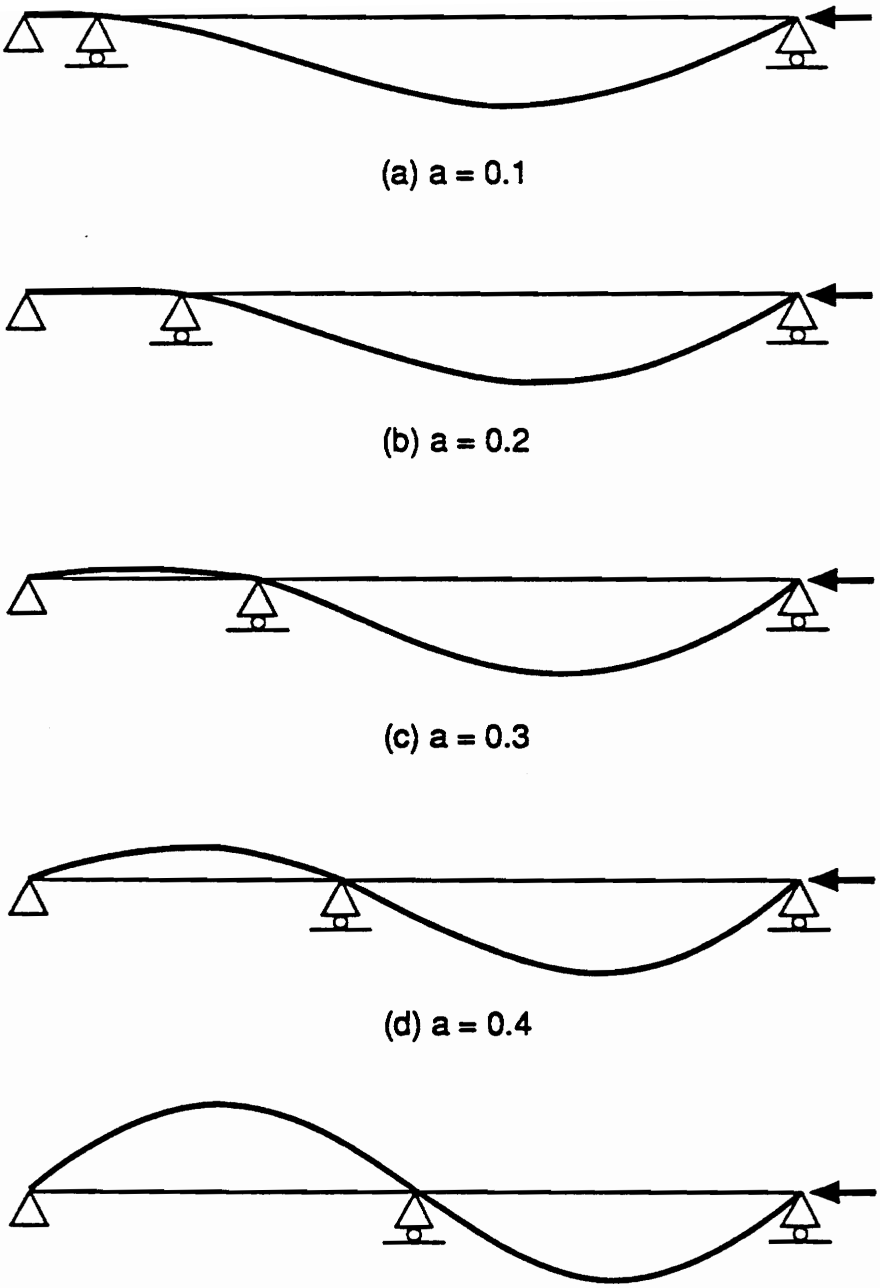

Figure 2.3 Buckling Mode Shapes for Different *a*'s

Table 1.2

Maximum Deflection of Each Span for Different *a*'s

a	w_{1m}	w_{10} at a	w_{2m}	w_{20} at 1
0.1	0.007	0.000	0.677	0.000
0.2	0.067	0.000	1.360	0.000
0.3	0.255	0.000	1.800	0.000
0.4	0.612	0.000	1.667	0.000
0.5	1.000	0.000	1.000	0.000

b. Case II : Simply Supported Column with One Intermediate Translational Spring

The boundary and transition conditions for this case are

$$w_1(0)=0, w_1''(0)=0$$

$$w_2(1)=0, w_2''(1)=0$$

$$w_1(a)=w_2(a), w_1'(a)=w_2'(a) \tag{2.1.9}$$

$$\gamma_2^2\, w_1''(a)=\gamma_1^2\, w_2''(a)$$

$$\gamma_1^2\, w_2'''(a)+\gamma_2^2\, k w_1(a)=\gamma_2^2\, w_1'''(a)$$

At x=*a*, the deflection, slope, and bending moment are continuous, and the difference in shear forces equals the spring force.

The characteristic equation for the buckling load is

$$\begin{aligned} f_1(\gamma_1,\gamma_2,k,a) \equiv \gamma_1^2(\gamma_2 \sin\gamma_1 a \cos\gamma_2 b \\ +\gamma_1 \cos\gamma_1 a \sin\gamma_2 b)+k(\sin\gamma_1 a \sin\gamma_2 b \\ -\gamma_1 ab \cos\gamma_1 a \sin\gamma_2 b-\gamma_2 ab \sin\gamma_1 a \cos\gamma_2 b)=0 \end{aligned} \tag{2.1.10}$$

where b=1-*a*.

If $\gamma_1=\gamma_2\equiv\gamma$, the characteristic equation can be written as

$$f_2(\gamma,k,a) \equiv \gamma^3 \sin\gamma+k(\sin\gamma a \sin\gamma b-\gamma ab \sin\gamma)=0 \tag{2.1.11}$$

where $p=\gamma^2$.

If *a*=0.5, Equation (2.1.11) can be written as

$$(\sin\frac{\gamma}{2})(2\gamma^3\cos\frac{\gamma}{2}+k\sin\frac{\gamma}{2}-k\frac{\gamma}{2}\cos\frac{\gamma}{2})=0 \tag{2.1.12}$$

In this research, k_{ideal} can be defined as the threshold of the spring stiffness k for which higher spring stiffnesses do not increase the critical load p_{cr}. Solutions of Equation (2.1.12) are

$$\sin\frac{\gamma}{2}=0 \tag{2.1.13}$$

and

$$(4\gamma^2-k)\gamma\cos\frac{\gamma}{2}+2k(\sin\frac{\gamma}{2})^2=0 \tag{2.1.14}$$

Equation (2.1.13) gives

$$\frac{\gamma}{2}=n\pi\rightarrow\gamma=2n\pi,\ (n=1,2,\cdots)$$

By putting $\gamma=2\pi$, the lowest of these values, into Equation (2.1.14), the ideal spring stiffness k_{ideal} can be obtained:

$$k_{ideal}=16\pi^2=157.91$$

However, there is no such k_{ideal} for other values of *a*. If $\gamma_1=\gamma_2$, k_{ideal} can only be obtained if the spans of the column are equal. Figure 2.4 shows the relation between p_{cr} and k for different *a*'s. If $a=0.5$ and $k>k_{ideal}$, the critical load is $p_{cr}=4\pi^2=39.478$. For the other values of *a*, p_{cr} increases as k increases and approaches the corresponding value in Table 1.1 (Case I) as $k\rightarrow\infty$.

For different values of *a*, Table 2.1 shows the spring stiffness k required for the critical

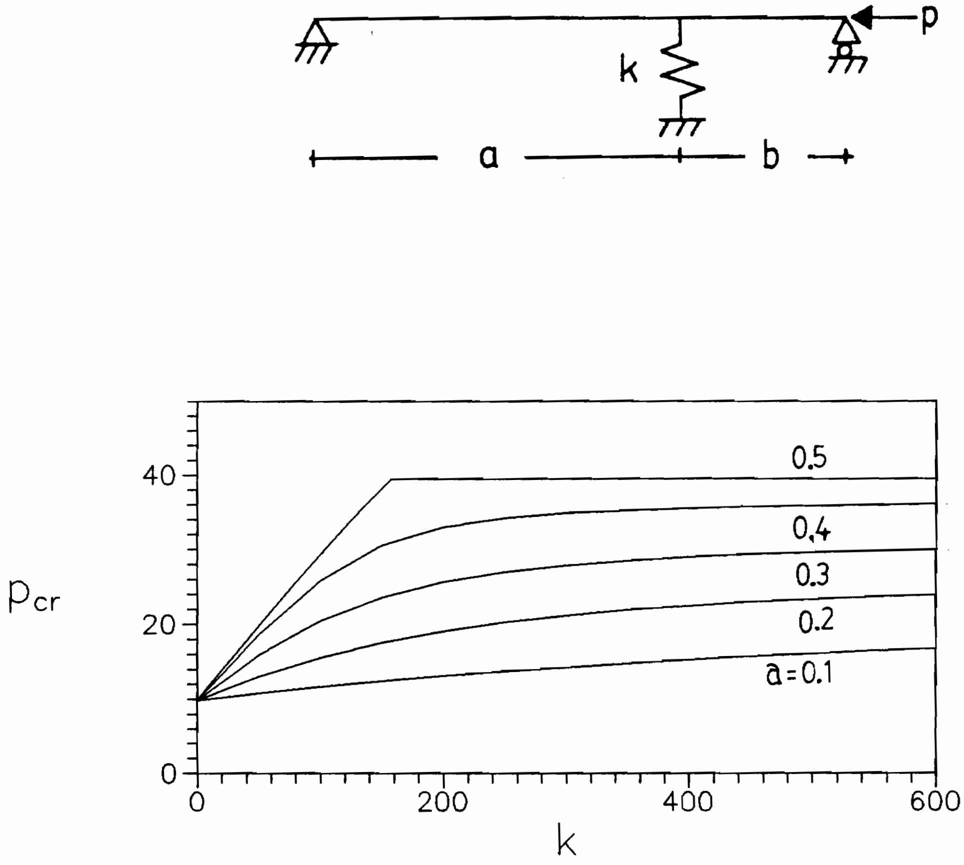

Figure 2.4 The Relation between p_{cr} and k for Different *a*'s

Table 2.1

Spring Stiffness k for which p_{cr} is a Given Percentage of p_{cr} for Case I

	0.1	0.2	0.3	0.4	0.5
75	703.776	251.334	154.675	115.975	101.702
80	970.170	331.192	193.737	135.590	112.538
85	1397.340	456.811	252.889	161.987	123.553
90	2225.750	696.705	362.222	205.248	134.769
95	4657.860	1393.350	672.251	315.772	146.212

load to be a certain percentage of the corresponding critical load in Case I. The formula for the spring stiffness k can be obtained directly from the characteristic equation:

$$k=-\frac{\gamma^3 \sin\gamma}{\sin\gamma a \sin\gamma b-\gamma ab \sin\gamma} \tag{2.1.15}$$

where $\gamma=\sqrt{p}$.

For example, if a=0.1, the critical load for Case I is 23.225 (Table 1.1). The value of k needed for p_{cr} in Case II to be 75% of that, i.e., 17.419, is found to be 703.80 by substituting p=17.419 into Equation (2.1.15).

Figure 2.5 shows the relation between p_{cr} and a for different k's. The curves are symmetric about a=0.5. If k=0, the critical load p_{cr} is that of a simply supported column ($p_{cr}=\pi^2$). For $k=\infty$, the curve is the same as in Figure 2.2 for Case I. Table 2.2 shows the critical load p_{cr} for k=50 and k=200, in which the span lengths a have various values.

The formulas of all the coefficients in terms of A_1 that are used to get the buckling modes are as follows:

$$A_2=0$$

$$A_3=(-\gamma_1 b \cos\gamma_1 a-\gamma_2 b \cot\gamma_2 b \sin\gamma_1 a)A_1$$

$$A_4=0$$

$$B_1=-\frac{\sin\gamma_1 a \cos\gamma_2}{\sin\gamma_2 b}A_1 \tag{2.1.16}$$

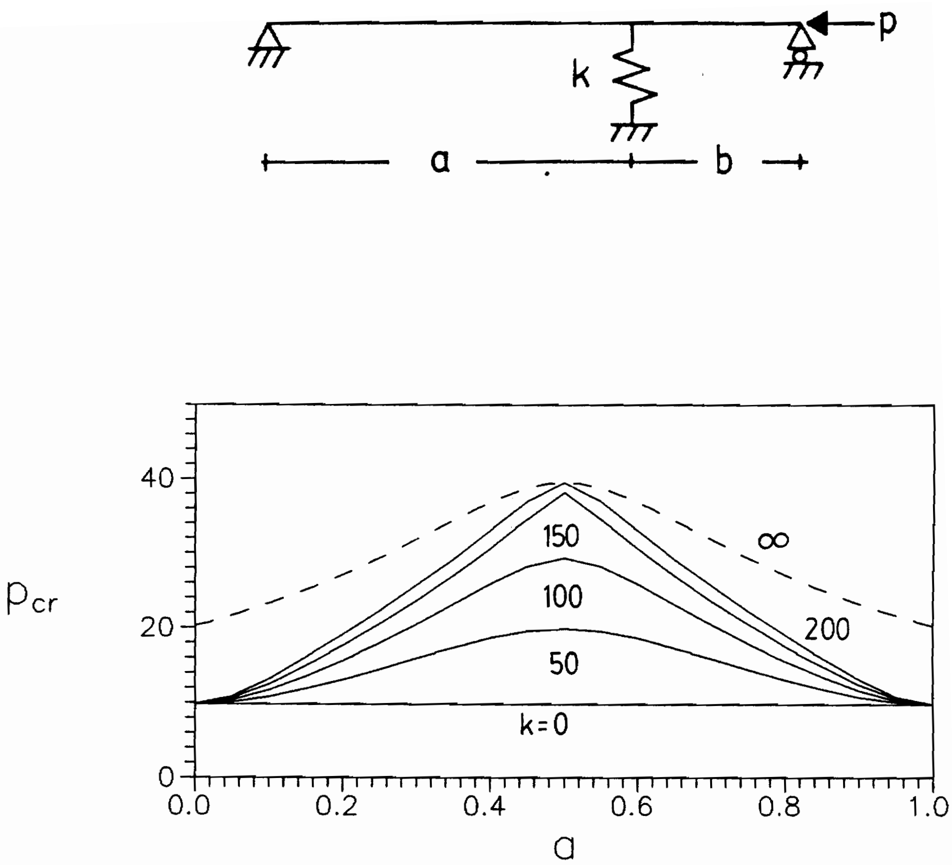

Figure 2.5 The Relation between p_{cr} and *a* for Different k's

Table 2.2

p_{cr} for Different *a*'s and k's

k \ $\bar{a}$	0.1	0.2	0.3	0.4	0.5
50	10.794	13.044	15.884	18.574	19.814
200	13.096	19.089	25.611	32.953	39.478

$$B_2 = \frac{\sin\gamma_1 a \; \sin\gamma_2}{\sin\gamma_2 b} A_1$$

$$B_3 = (\gamma_1 a \; \cos\gamma_1 a + \gamma_2 a \; \cot\gamma_2 b \; \sin\gamma_1 a) A_1$$

$$B_4 = -B_3$$

Figure 2.6 shows the buckling mode shapes for k=200. If a=0.5 and k>k_{ideal}, as in Figure 2.6, the mode is a sine curve as seen before in Case I. The modes for a>0.5 can be obtained by symmetry. Table 2.3 and Table 2.4 show the values of w_{1m} and w_{2m} for different a's with k=50 and k=200, respectively.

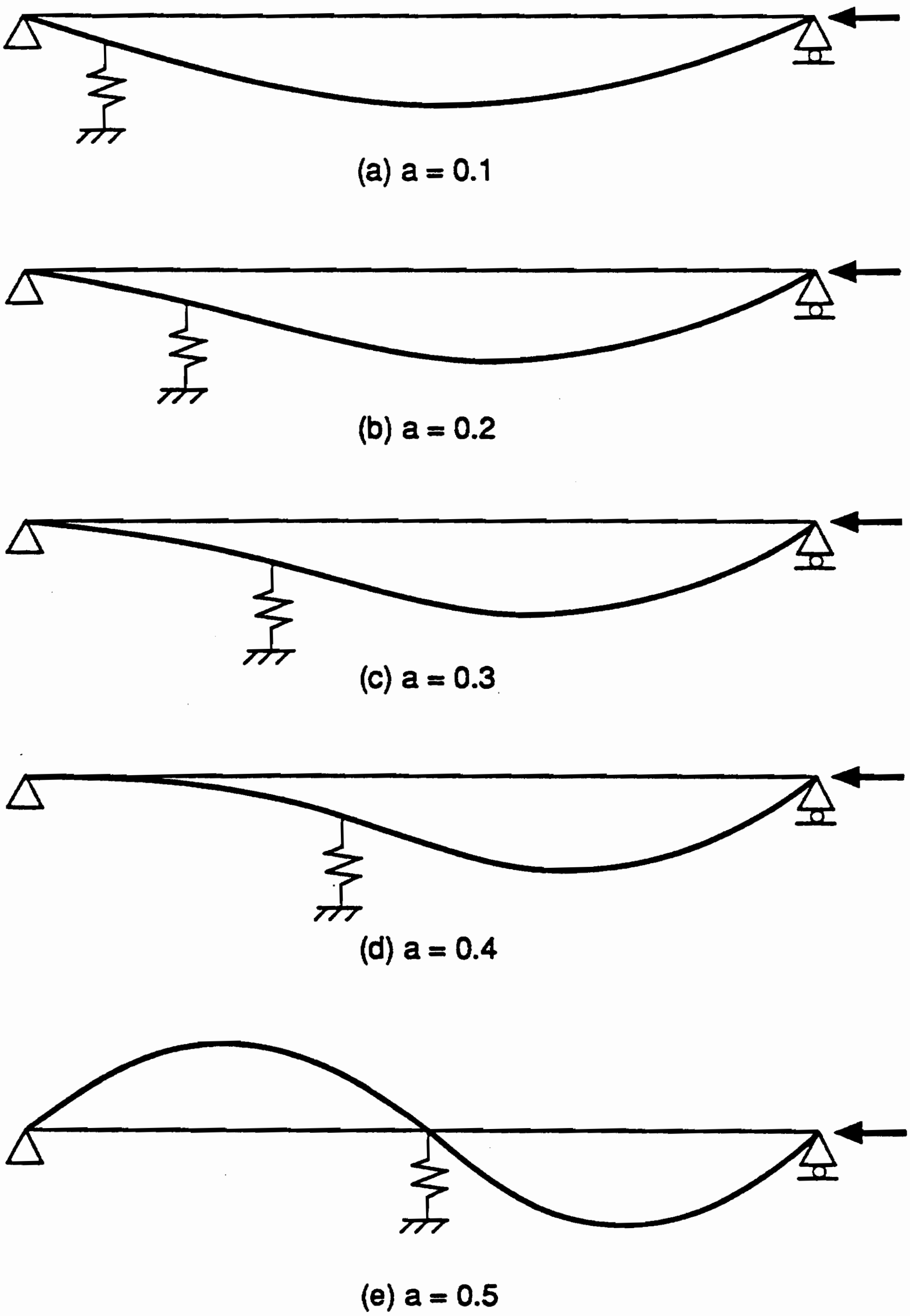

Figure 2.6 Buckling Mode Shapes for k=200

Table 2.3

Maximum Deflection of Each Span for Different *a*'s with k=50

a	w_{1m}	w_{10} at *a*	w_{2m}	w_{20} at 1
0.1	0.553	0.553	1.881	0.000
0.2	1.709	1.709	3.243	0.000
0.3	2.745	2.745	3.800	0.000
0.4	2.792	2.792	3.101	0.000
0.5	2.148	2.148	2.149	0.000

Table 2.4

Maximum Deflection of Each Span for Different *a*'s with k=200

a	w_{1m}	w_{10} at *a*	w_{2m}	w_{20} at 1
0.1	0.945	0.945	3.727	0.000
0.2	1.134	1.134	3.135	0.000
0.3	1.561	1.561	3.796	0.000
0.4	1.639	1.639	3.695	0.000
0.5	1.000	0.000	1.000	0.000

c. <u>Case III : Column with One End Hinged and Two Translational Springs</u>

The boundary and transition conditions for this column are

$$w_1(0)=0,\; w_1''(0)=0$$

$$w_1(a)=w_2(a),\; w_1'(a)=w_2'(a)$$

$$\gamma_2^2 w_1''(a)=\gamma_1^2 w_2''(a)$$

$$\gamma_1^2 w_2'''(a)+\gamma_2^2 k_1 w_1(a)=\gamma_2^2 w_1'''(a) \tag{2.1.17}$$

$$w_2''(1)=0$$

$$\gamma_1^2 w_2'''(1)+\gamma_1^2\gamma_2^2 w_2'(1)=\gamma_2^2 k_2 w_2(1)$$

The characteristic equation for the buckling loads is

$$\begin{aligned}
&f_1(\gamma_1,\gamma_2,k_1,k_2,a)\\
&\equiv(\gamma_1^2-k_2)\,[-\frac{\gamma_1^2}{k_1 a}(\gamma_2 \sin\gamma_1 a \cos\gamma_2 b+\gamma_1 \cos\gamma_1 a \sin\gamma_2 b)\\
&-\frac{1}{a} \sin\gamma_1 a \sin\gamma_2 b+\gamma_1 \cos\gamma_1 a \sin\gamma_2 b\\
&+\gamma_2 \sin\gamma_1 a \cos\gamma_2 b]+k_2(\gamma_1 a \cos\gamma_1 a \sin\gamma_2 b\\
&+\gamma_2 a \cos\gamma_2 b \sin\gamma_1 a)=0
\end{aligned} \tag{2.1.18}$$

If $\gamma_1=\gamma_2\equiv\gamma$, the characteristic equation can be written as

$$f_2(\gamma, k_1, k_2, a)$$
$$\equiv(\gamma^2-k_2)\left(-\frac{\gamma^3}{k_1 a}\sin\gamma+\gamma\sin\gamma-\frac{1}{a}\sin\gamma a\sin\gamma b\right) \tag{2.1.19}$$
$$+k_2\gamma a\sin\gamma=0$$

where p= γ^2.

If a=0.5 and $k_1=k_2\equiv k$, Equation (2.1.19) can be written as

$$\left(\sin\frac{\gamma}{2}\right)\left[(\gamma^2-k)\left(-\frac{4\gamma^3}{k}\cos\frac{\gamma}{2}+2\gamma\cos\frac{\gamma}{2}-2\sin\frac{\gamma}{2}\right)+k\gamma\cos\frac{\gamma}{2}\right]=0. \tag{2.1.20}$$

Solutions of Equation (2.1.20) are

$$\sin\frac{\gamma}{2}=0 \tag{2.1.21}$$

and

$$\left[(\gamma^2-k)\left(-\frac{4\gamma^3}{k}\cos\frac{\gamma}{2}+2\gamma\cos\frac{\gamma}{2}-2\sin\frac{\gamma}{2}\right)+k\gamma\cos\frac{\gamma}{2}\right]=0 \tag{2.1.22}$$

Equation (2.1.21) gives

$$\frac{\gamma}{2}=n\pi\rightarrow\gamma=2n\pi,\ (n=1,2,\cdots)$$

At $\gamma=2n\pi$, Equation (2.1.22) gives

$$(\cos n\pi)\left[(\gamma^2-k)\left(-\frac{4\gamma^3}{k}+2\gamma\right)+k\gamma\right]=0$$

which leads to

$$k^2-6\gamma^2k+4\gamma^4=0 \tag{2.1.23}$$

From Equation (2.1.23), k can be obtained for $\gamma=2n\pi$ as follows:

$$k=4n^2\pi^2(3\pm\sqrt{5})$$

Then

k=30.1588 or k=206.7117 for n=1.

As defined in Case II, k_{ideal} is the required spring stiffness for which higher spring stiffnesses k do not increase the critical load p_{cr}. For k<206.7117, Equation (2.1.22) has a root γ that is lower than 2π, but for k>206.7117 it does not. Therefore

k_{ideal}=206.7117.

As for Case II, there is no k_{ideal} when $\gamma_1=\gamma_2$ except for a=0.5.

Figure 2.7 shows the relation between p_{cr} and k for different a's. If a=0.5 and $k>k_{ideal}$, the critical load is $p_{cr}=4\pi^2$=39.478. If a<0.5, p_{cr} is higher when the internal spring is at x=a than when it is at x=1- a(e.g., it is higher for a=0.4 than for a=0.6), although both cases have the same p_{cr} at k=0 and in the limit as $k\to\infty$. Table 3.1 shows the spring stiffness k required for the critical load to be a certain percentage of the corresponding critical load in Case I.

The formula for the spring stiffness k can be obtained from the characteristic equation written in the form

$$Dk^2+Ek+F=0.$$

Then

$$k=\frac{-E\pm\sqrt{H}}{2D} \tag{2.1.24}$$

where

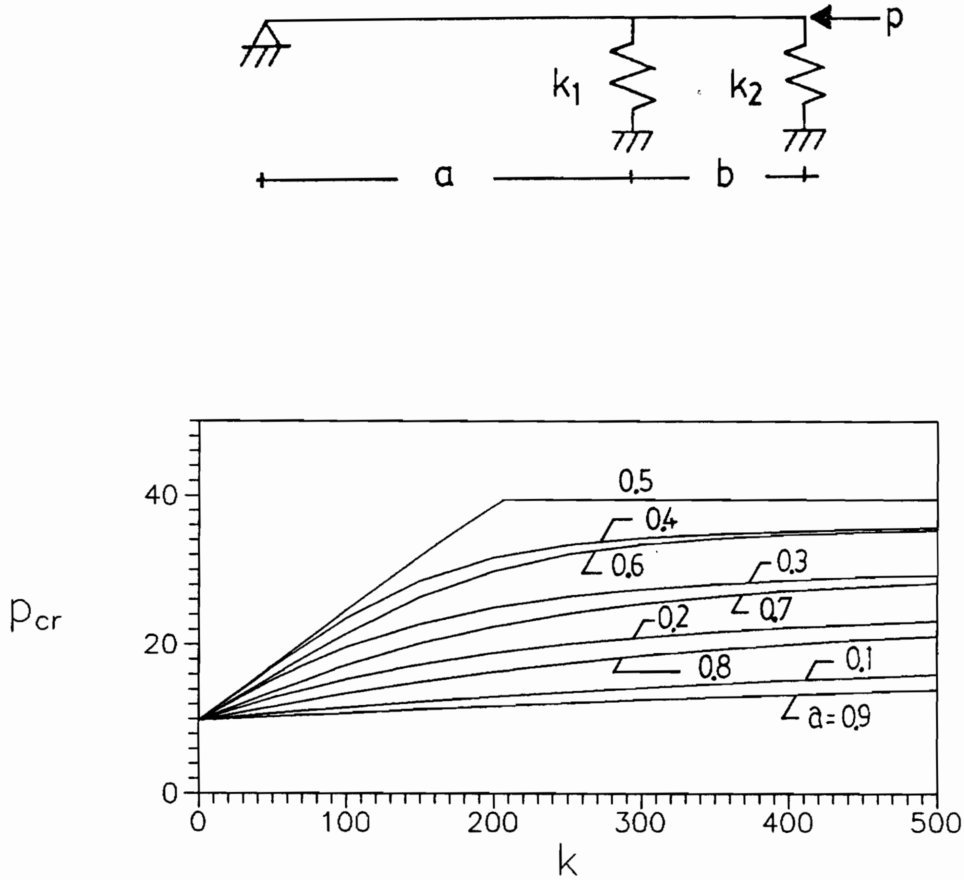

Figure 2.7 The Relation between p_{cr} and k for Different *a*'s

Table 3.1

Spring Stiffness k for which p_{cr} is a Given Percentage of p_{cr} for Case I

% \ a	0.1	0.2	0.3	0.4	0.5	0.6	0.7	0.8	0.9
75	710.9	262.2	170.9	139.1	134.3	166.1	238.9	420.3	1281.
80	980.1	345.3	231.5	162.1	148.3	193.2	297.5	551.8	1764.
85	1411.	476.0	278.1	192.9	162.4	229.5	386.1	758.3	2538.
90	2248.	725.5	397.3	243.2	176.9	288.7	549.5	1152.	4037.
95	4704.	1450.	735.3	371.5	191.7	439.3	1011.	2295.	8440.

$$D=\gamma\ \sin\gamma-\frac{1}{a}\ \sin\gamma a\ \sin\gamma b-\gamma a\ \sin\gamma$$

$$E=-\gamma^2(\gamma\ \sin\gamma-\frac{1}{a}\ \sin\gamma a\ \sin\gamma b+\frac{\gamma}{a}\ \sin\gamma)$$

$$F=\frac{\gamma^5}{a}\sin\gamma$$

$$H=E^2-4DF$$

$$\gamma=\sqrt{p}\ .$$

In the figures, $\gamma_1=\gamma_2\equiv\gamma$ and $k_1=k_2\equiv k$.

Figure 2.8 presents the critical load p_{cr} as a function of a with fixed k's. If $k\to\infty$, the critical loads p_{cr} are the same as for Case I except at $a=0$ and $a=1$. As $a\to 1$, Equation (2.1.19) with $k_1=k_2\equiv k$ can be written as

$$\gamma\ \sin\gamma[k^2-(\gamma^2-k)^2]=0$$

Then the following relation can be obtained:

if $k\leq\pi^2/2$, $p_{cr}\to 2k$ as $a\to 1$

if $k\geq\pi^2/2$, $p_{cr}\to\pi^2$ as $a\to 1$

To get p_{cr} as $a\to 0$, Equation (2.1.19) with $k_1=k_2\equiv k$ can be multiplied by a and then one can set $a=0$. This leads to the following result:

if $k\leq\pi^2$, $p_{cr}\to k$ as $a\to 0$

if $k\geq\pi^2$, $p_{cr}\to\pi^2$ as $a\to 0$

If k is sufficiently large, the maximum critical load occurs when the internal spring is near

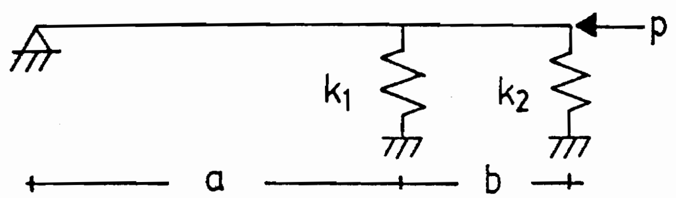

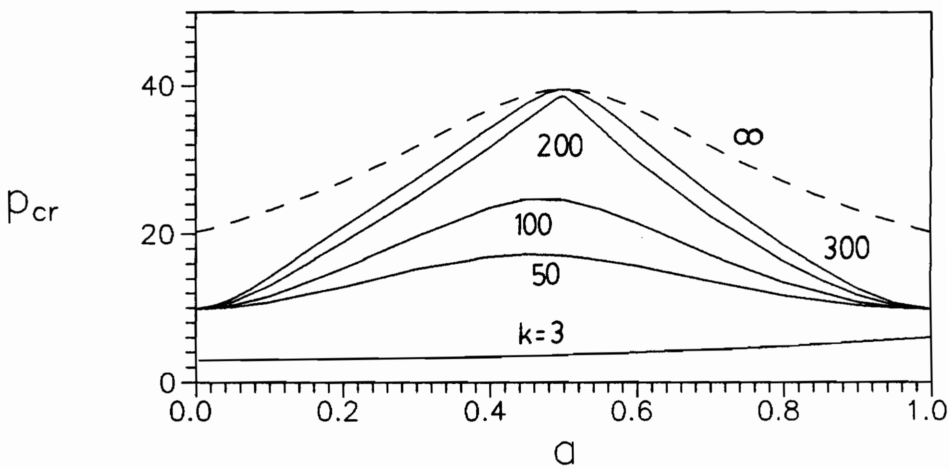

Figure 2.8 p_{cr} for Different *a*'s with Fixed k's

the center of the column, with a slightly less than 0.5. If k is small enough, the critical load increases as a increases. For k=3 in Figure 2.8, $p_{cr} \to 6$ as $a \to 1$, while $p_{cr} \to \pi^2$ for the other curves shown. Table 3.2 shows the critical load p_{cr} for different a's and k's.

The formulas of all the coefficients in terms of A_1 that are used to get the buckling modes are as follows:

$$A_2 = 0$$

$$A_3 = -\frac{1}{k_1 a}[\gamma_1^3 \cos\gamma_1 a + k_1 \sin\gamma_1 a + \gamma_2\gamma_1^2 \sin\gamma_1 a \cot\gamma_2 b]A_1$$

$$A_4 = 0$$

$$B_1 = -\frac{\sin\gamma_1 a \cos\gamma_2}{\sin\gamma_2 b}A_1 \qquad (2.1.25)$$

$$B_2 = \frac{\sin\gamma_1 a \sin\gamma_2}{\sin\gamma_2 b}A_1$$

$$B_3 = [\cos\gamma_1 a(\gamma_1 - \frac{\gamma_1^3}{k_1 a}) + \frac{\sin\gamma_1 a}{\tan\gamma_2 b}(\gamma_2 - \frac{\gamma_2\gamma_1^2}{k_1 a}) - \frac{1}{a}\sin\gamma_1 a]A_1$$

$$B_4 = [-\gamma_1 a \cos\gamma_1 a - \gamma_2 a \cos\gamma_2 b \frac{\sin\gamma_1 a}{\sin\gamma_2 b}]A_1$$

The buckling mode shapes are presented in Figure 2.9 for k=300. If a=0.5 and $k \geq k_{ideal}$, the buckling mode shape is a sine curve as before. Table 3.3, Table 3.4, and Table 3.5 show the values of w_{1m} and w_{2m} for different a's with k=50, k=200, and k=300, respectively.

Table 3.2

p_{cr} for Different *a*'s and k's

k \ a	0.1	0.2	0.3	0.4	0.5	0.6	0.7	0.8	0.9
3	3.0	3.1	3.3	3.4	3.7	4.0	4.4	4.8	5.4
50	10.8	12.9	15.3	17.0	17.1	15.7	13.6	11.7	10.3
200	13.1	18.9	25.0	31.6	38.6	30.0	22.4	16.4	11.8
300	14.3	21.0	27.4	34.2	39.5	33.4	25.5	18.5	12.6

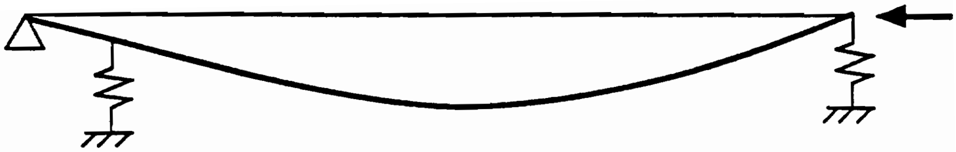

(a) a = 0.1

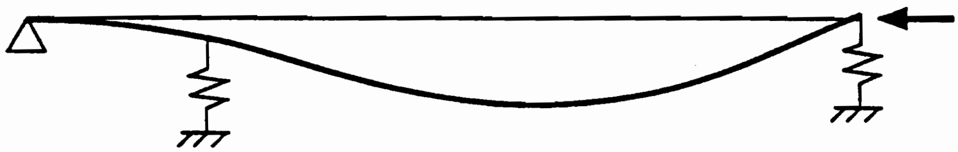

(b) a = 0.2

(c) a = 0.3

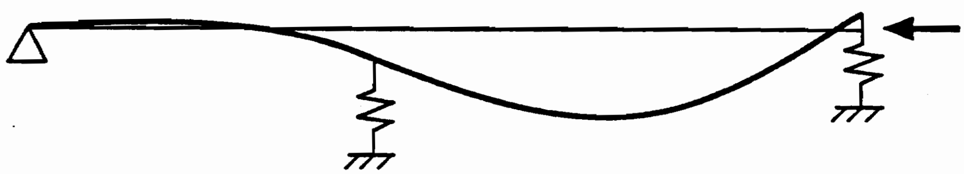

(d) a = 0.4

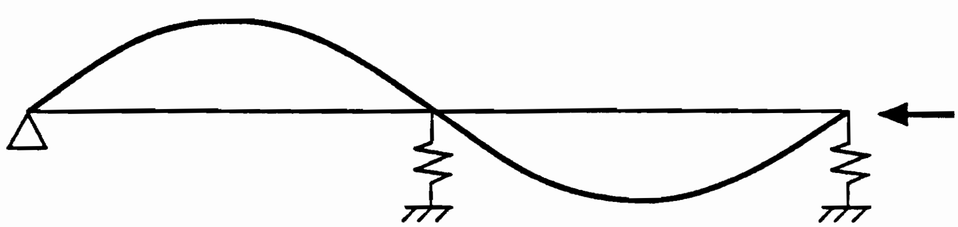

(e) a = 0.5

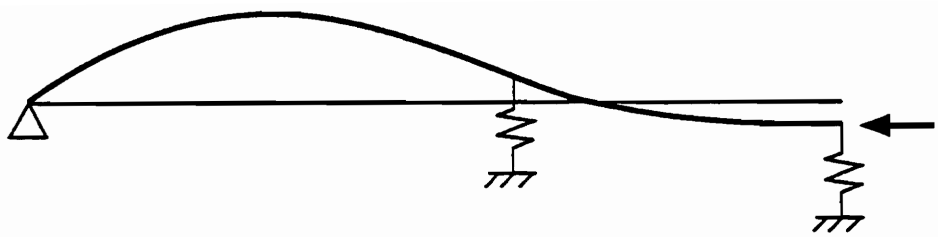

(f) a = 0.6

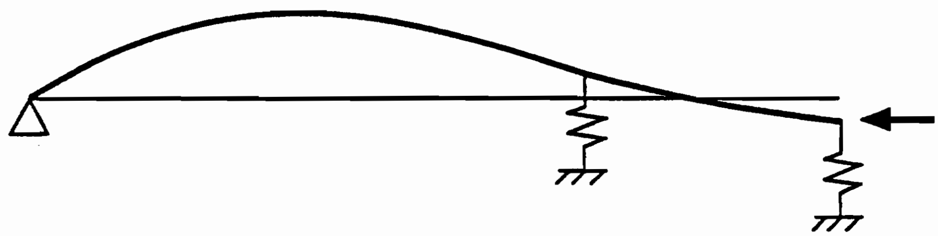

(g) a = 0.7

(h) a = 0.8

(i) a = 0.9

Figure 2.9 Buckling Mode Shapes for k=300

Table 3.3

Maximum Deflection of Each Span for Different *a*'s with k=50

a	w_{1m}	w_{10} at *a*	w_{2m}	w_{20} at 1
0.1	0.542	0.542	1.830	0.069
0.2	1.518	1.518	2.804	0.409
0.3	2.087	2.087	2.737	0.901
0.4	1.864	1.864	1.953	1.129
0.5	1.386	1.352	1.352	1.028
0.6	1.148	0.910	0.910	0.796
0.7	1.035	0.587	0.587	0.564
0.8	0.970	0.345	0.360	0.360
0.9	0.951	0.155	0.176	0.176

Table 3.4

Maximum Deflection of Each Span for Different *a*'s with k=200

a	w_{1m}	w_{10} at *a*	w_{2m}	w_{20} at 1
0.1	0.964	0.964	3.780	0.103
0.2	1.170	1.170	3.156	0.258
0.3	1.720	1.720	3.919	0.590
0.4	2.372	2.372	4.492	1.127
0.5	2.501	2.397	2.397	1.485
0.6	1.449	0.730	0.730	0.514
0.7	1.359	0.537	0.537	0.423
0.8	1.229	0.359	0.324	0.312
0.9	1.059	0.170	0.162	0.162

Table 3.5

Maximum Deflection of Each Span for Different *a*'s with k=300

a	w_{1m}	w_{10} at *a*	w_{2m}	w_{20} at 1
0.1	0.418	0.418	1.807	0.044
0.2	0.637	0.637	2.184	0.137
0.3	0.832	0.832	2.719	0.275
0.4	0.778	0.778	2.540	0.351
0.5	1.000	0.000	1.000	0.000
0.6	1.359	0.423	0.423	0.285
0.7	1.374	0.405	0.405	0.301
0.8	1.296	0.320	0.287	0.273
0.9	1.111	0.169	0.159	0.158

d. Case IV : Column with One Rotational Spring and Two Translational Springs

The boundary conditions for this column are

$$w_1(0)=0, w_1''(0)-cw_1'(0)=0$$

$$w_1(a)=w_2(a), w_1'(a)=w_2'(a)$$

$$\gamma_2^2 w_1''(a)=\gamma_1^2 w_2''(a) \tag{2.1.26}$$

$$\gamma_1^2 w_2'''(a)+\gamma_2^2 k_1 w_1(a)=\gamma_2^2 w_1'''(a)$$

$$w_2''(1)=0$$

$$\gamma_1^2 w_2'''(1)+\gamma_1^2\gamma_2^2 w_2'(1)=\gamma_2^2 k_2 w_2(1)$$

The characteristic equation for the buckling loads is

$$\begin{aligned}[H_{15}+(H_1+H_2H_{14})H_{16}+H_{14}\gamma_1^2\gamma_2\cos\gamma_2 a-H_7H_{14}\gamma_1^2\gamma_2\sin\gamma_2 a \\ -(H_5+H_6H_{14})k_1 a-(H_3+H_4H_{14})k_1]=0\end{aligned} \tag{2.1.27}$$

Each variable used in the above equation is given in the Appendix. In the figures, $\gamma_1=\gamma_2\equiv\gamma$ and $k_1=k_2\equiv k$.

Figure 2.10 shows the effects of the rotational spring stiffness c on p_{cr} as a function of a with k=200. If c=0, the result is exactly the same for k=200 as shown in Figure 2.8 for Case III. If $c\rightarrow\infty$, the end x=0 is a fixed end. As c increases, the value of a giving the maximum p_{cr} increases from $a\approx0.5$ to $a\approx0.6$. Table 4.1 shows the critical load p_{cr} for

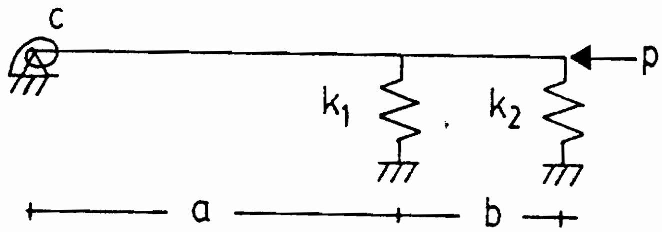

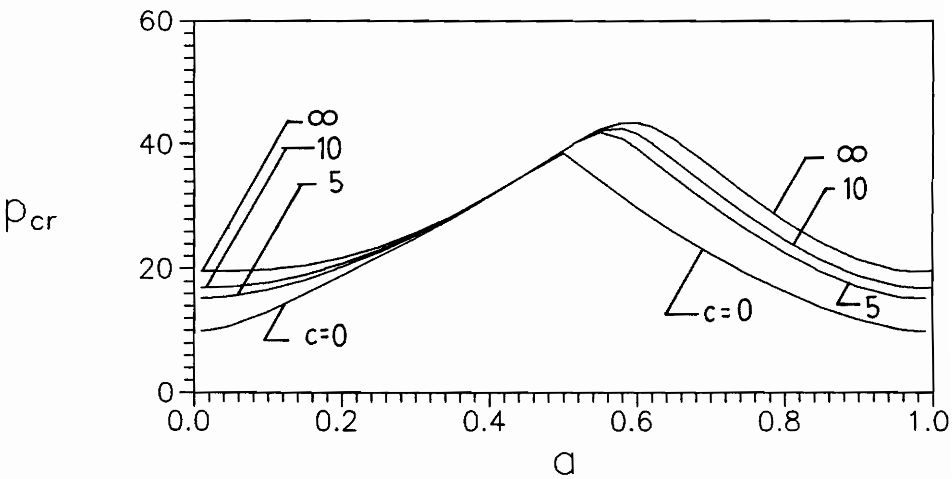

Figure 2.10 p_{cr} **for Different** ***a*****'s and c's with k=200**

Table 4.1

p_{cr} for Different *a*'s and c's with k=200

c \ a	0.1	0.2	0.3	0.4	0.5	0.6	0.7	0.8	0.9
0	13.1	18.9	25.0	31.6	38.6	29.8	22.4	16.4	11.8
5	16.6	20.3	25.4	31.7	39.0	39.3	30.3	22.7	17.1
10	17.8	20.8	25.5	31.7	39.0	41.7	32.9	24.7	18.9
∞	19.8	21.7	25.7	31.7	39.0	43.5	36.5	27.8	21.5

different a's and c's with k=200.

Figure 2.11 shows the effects of the translational spring stiffness k on p_{cr} as a function of a when c=10. The curve k=200 in Figure 2.11 is the same as the curve c=10 in Figure 2.10. The value of a for maximum p_{cr} tends to increase as k increases. Table 4.2 shows the critical load p_{cr} for different a's and k's with c=10.

In Case IV, there are no values c_{ideal} and k_{ideal}. Figure 2.12 shows the relation between p_{cr} and k for fixed values of c and a, and Figure 2.13 shows p_{cr} versus c for fixed values of k and a.

In order to show the effect of a support that stiffens as it is compressed, the rotational spring stiffness c is assumed to be proportional to p [9]:

$$c=g\gamma^2 \tag{2.1.28}$$

If c=0 or c=∞, the support at x=0 is considered as an ideal pinned end or an ideal clamped end, respectively. As the applied load p increases, the resistance to rotation increases. Figure 2.14 shows the effects of the stiffening rate g for several k's when a=0.5, and Figure 2.15 shows the effect of a for different k's when g=0.1.

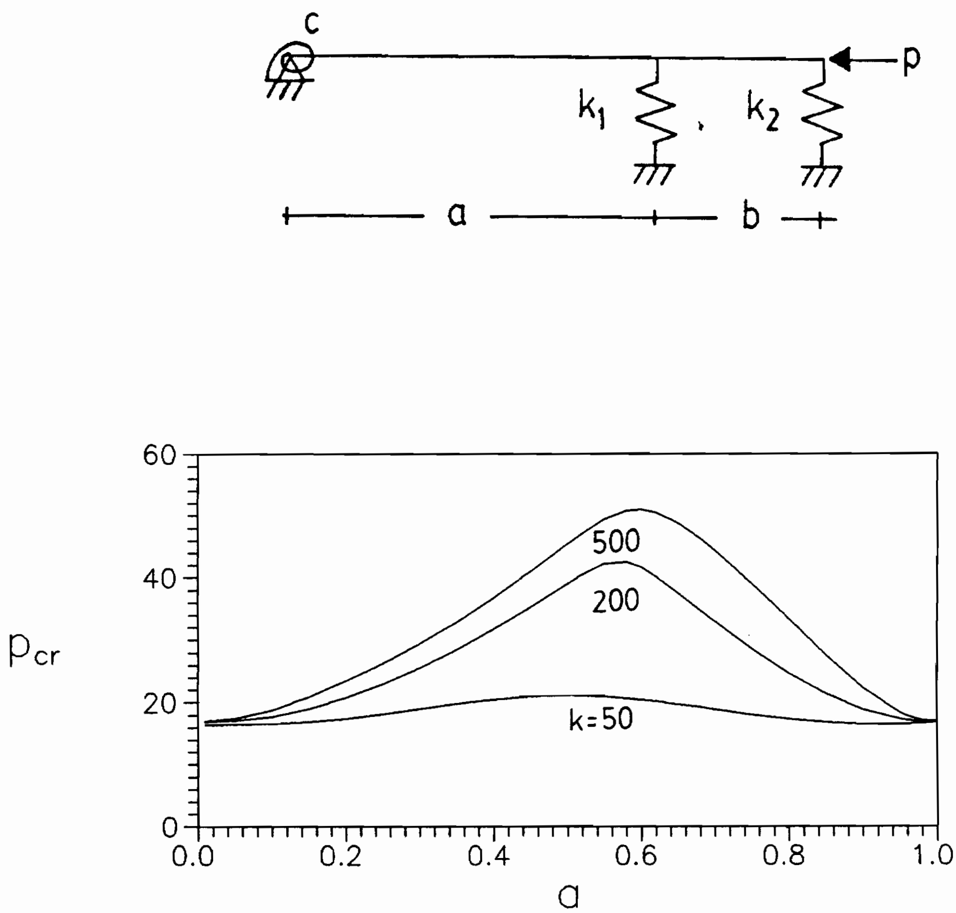

Figure 2.11 p_{cr} for Different *a*'s and k's with c=10

Table 4.2

p_{cr} for Different *a*'s and k's with c=10

k \ a	0.1	0.2	0.3	0.4	0.5	0.6	0.7	0.8	0.9
50	16.6	17.5	19.0	20.5	21.2	20.5	18.9	17.3	16.6
200	17.8	20.8	25.5	31.7	39.0	41.7	32.9	24.8	18.8
500	18.8	23.4	29.4	36.7	45.5	50.9	44.3	33.4	22.3

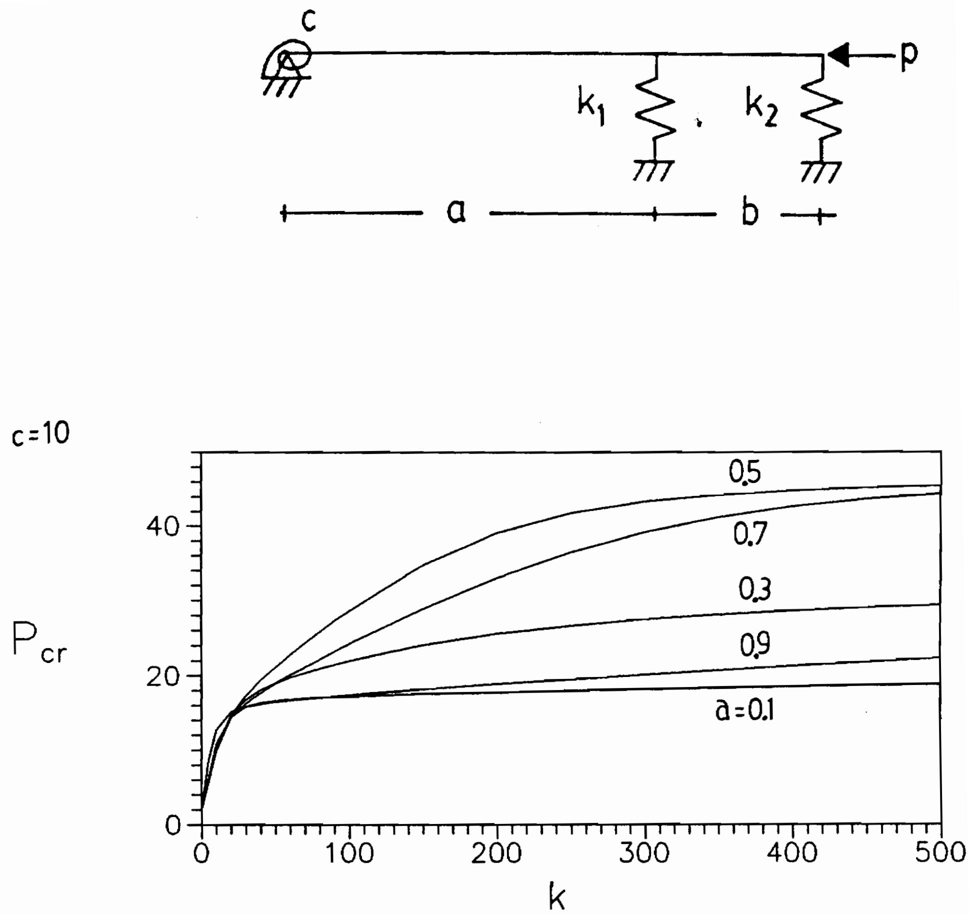

Figure 2.12 p_{cr} **for Different k's with Fixed c's and a's**

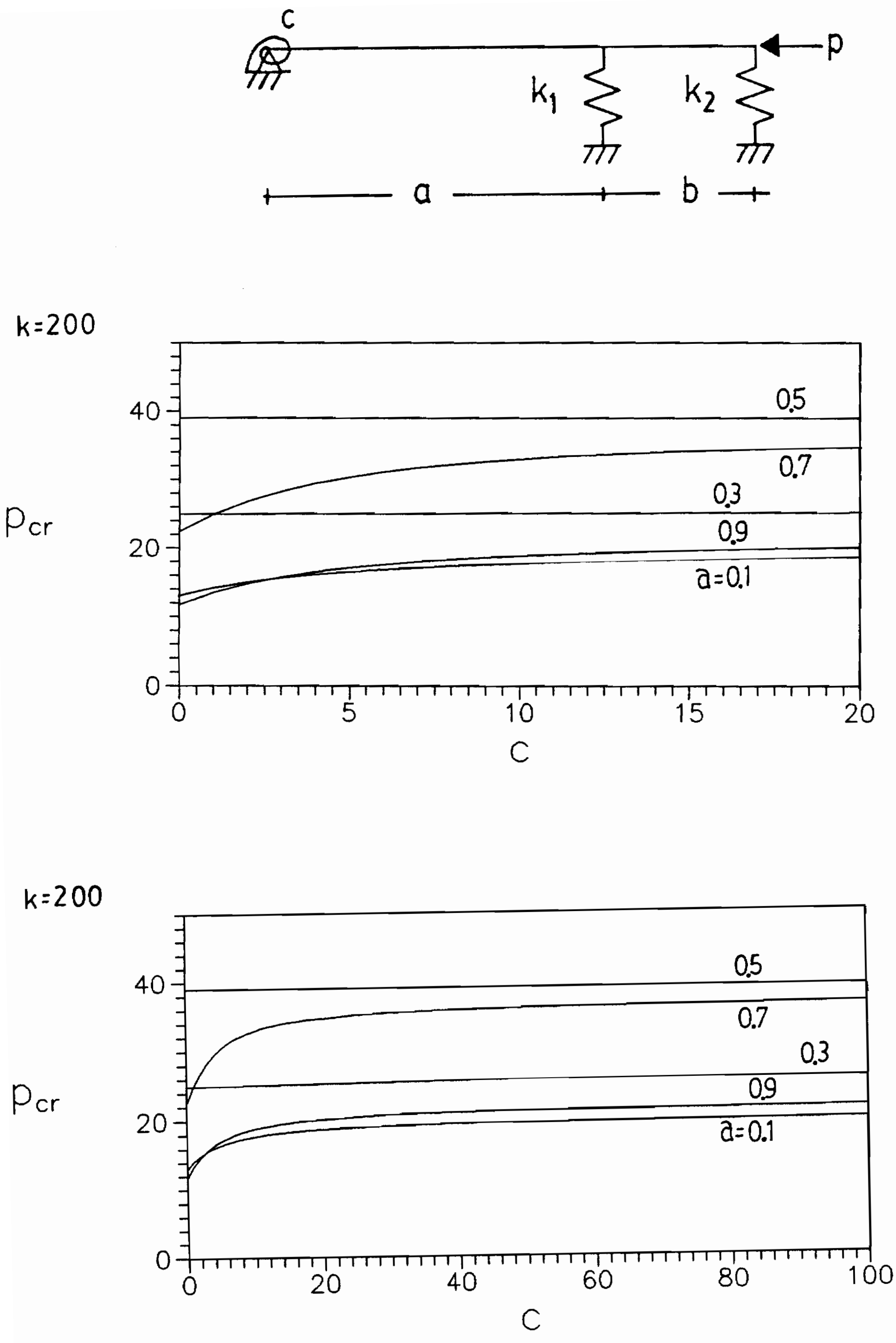

Figure 2.13 p_{cr} for Fixed k's and *a*'s with Different c

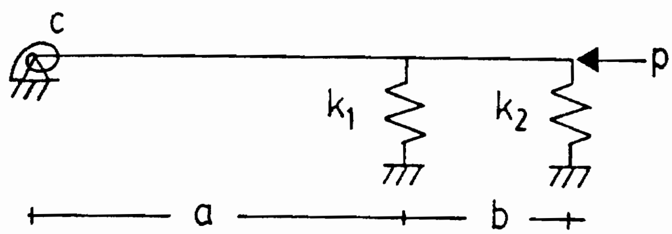

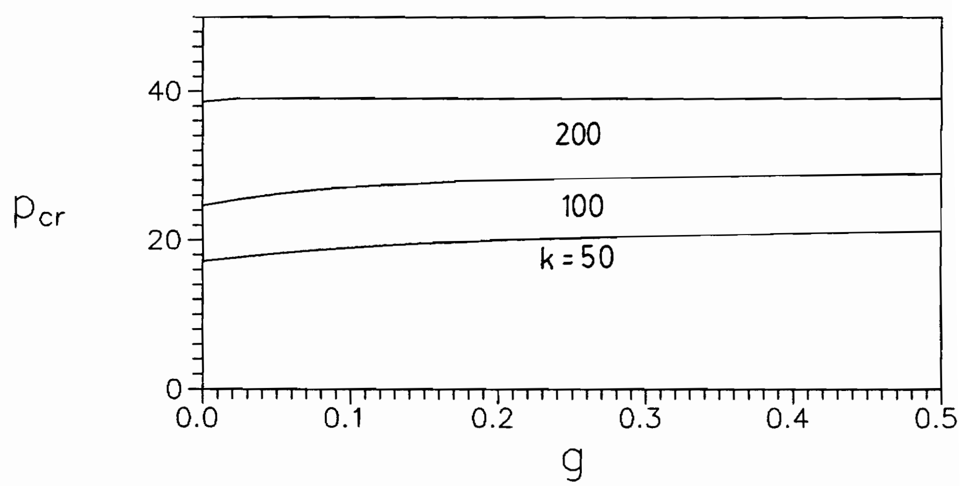

Figure 2.14 p_{cr} versus g for Several k's with a=0.5

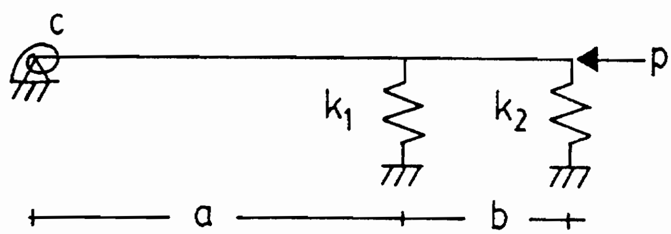

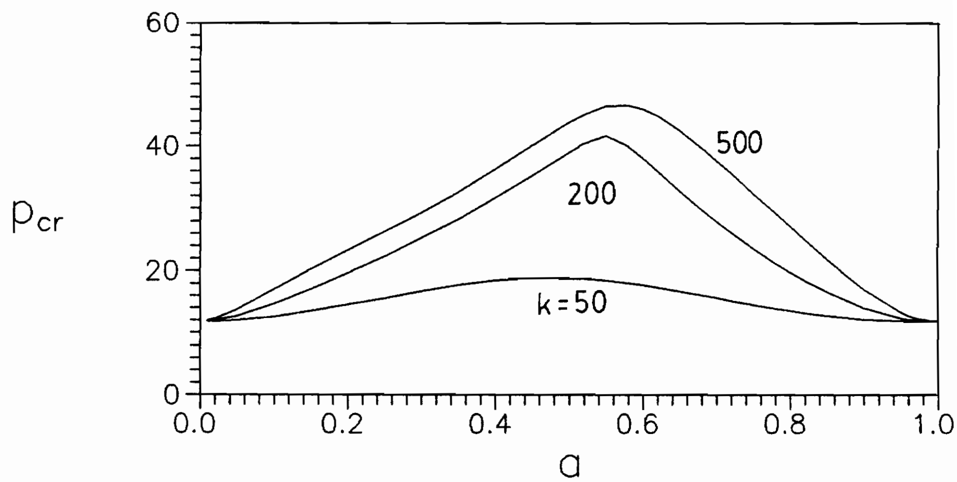

Figure 2.15 p_{cr} for Different k's with g=0.1

2.2 Imperfect Columns

In this section, an imperfect column will be analyzed for various span lengths $\bar{a}$ and $\bar{b}$. One purpose of this investigation is to find the reaction forces $\bar{R}_2$ and $\bar{R}_3$ at $\bar{x}=\bar{a}$ and $\bar{x}=L$, respectively, until the axial compressive load P reaches the critical load P_{cr} for the previous perfect column. Another purpose of this investigation is to find the maximum deflection of each column. The initial deflection of each column (when P=0) has the shape of the buckling mode of the corresponding perfect column and has a specified size. Since the reaction forces and the deflections are proportional to the initial deflection, results for initial deflections of the same shape but another magnitude can be obtained directly from the results to be presented here.

Since imperfect columns are related to the previous perfect columns, several coefficients that were used to get the buckling modes in the previous perfect columns are also used here, and are now denoted as $\tilde{A}_i$ and $\tilde{B}_i$, (i=1,··,4). The critical loads for the previous perfect columns are denoted β_1^2 and β_2^2 in this section. The relation between β_i and γ_i, (i=1,2), can be written as $\beta_1/\beta_2=\gamma_1/\gamma_2$.

In each case, the column under consideration may have different bending stiffnesses EI_i, (i=1,2), in each span, and the column is subjected to an axial compressive load P. The initial shape of the column is $\bar{w}_{10}(\bar{x})$ for $0\leq\bar{x}\leq\bar{a}$ and $\bar{w}_{20}(\bar{x})$ for $\bar{a}\leq\bar{x}\leq L$.

The equilibrium equations for each case are

$$EI_1\bar{w}_1^{////}(\bar{x})+P\bar{w}_1^{//}(\bar{x})=EI_1\bar{w}_{10}^{////}(\bar{x}),\ (0\leq\bar{x}\leq\bar{a})$$

and (2.2.1)

$$EI_2\bar{w}_2^{////}(\bar{x})+P\bar{w}_2^{//}(\bar{x})=EI_2\bar{w}_{20}^{////}(\bar{x}),\ (\bar{a}\leq\bar{x}\leq L)$$

For simplicity, nondimensional quantities are defined as follows:

$$x=\frac{\bar{x}}{L},\ a=\frac{\bar{a}}{L}$$

$$b=1-a$$

$$w_{10}=\frac{\bar{w}_{10}}{L},\ w_{20}=\frac{\bar{w}_{20}}{L}$$

$$w_1=\frac{\bar{w}_1}{L},\ w_2=\frac{\bar{w}_2}{L}$$

$$\gamma_1=\sqrt{\frac{PL^2}{EI_1}},\ \gamma_2=\sqrt{\frac{PL^2}{EI_2}} \tag{2.2.2}$$

$$k_1=\frac{\bar{k}_1L^3}{EI_1},\ k_2=\frac{\bar{k}_2L^3}{EI_1}$$

$$k=\frac{\bar{k}L^3}{EI_1},\ p=\frac{PL^2}{EI_1}$$

$$R_2=\frac{\bar{R}_2L^2}{EI_1},\ R_3=\frac{\bar{R}_3L^2}{EI_1}$$

Then the equilibrium equations and general solutions for each case can be written as

$$w_1^{////}(x)+\gamma_1^2\, w_1^{//}(x)=w_{10}^{////}(x)$$

$$w_1(x)=C_1\sin\gamma_1x+C_2\cos\gamma_1x+C_3x+C_4+W\sin\beta_1x,\ (0\le x\le a) \tag{2.2.3}$$

and

$$w_2^{''''}(x)+\gamma_2^2 w_2^{''}(x)=w_{20}^{''''}(x)$$

$$w_2(x)=D_1\sin\gamma_2 x+D_2\cos\gamma_2 x+D_3 x+D_4+Y\sin\beta_2 x+Z\cos\beta_2 x,\ (a\le x\le 1) \tag{2.2.4}$$

where

$$w_{10}(x)=\tilde{A}_1\sin\beta_1 x+\tilde{A}_3 x$$

$$w_{20}(x)=\tilde{B}_1\sin\beta_2 x+\tilde{B}_2\cos\beta_2 x+\tilde{B}_3 x+\tilde{B}_4$$

$$W=\frac{\tilde{A}_1\beta_1^2}{(\beta_1^2-\gamma_1^2)}$$

$$Y=\frac{\tilde{B}_1\beta_2^2}{(\beta_2^2-\gamma_2^2)}$$

$$Z=\frac{\tilde{B}_2\beta_2^2}{(\beta_2^2-\gamma_2^2)}$$

In all the numerical results to be presented, the column is assumed to be uniform ($EI_1=EI_2$, $\gamma_1=\gamma_2\equiv\gamma$, $\beta_1=\beta_2$) and the spring constants k_1 and k_2 in Case VII are assumed to be equal ($k_1=k_2\equiv k$).

a. <u>Case V : Case I with Initial Deflection</u>

The boundary and transition conditions for Case V are

$$w_1(0)=0,\, w_1''(0)-w_{10}''(0)=0$$

$$w_2(1)=0,\, w_2''(1)-w_{20}''(1)=0$$

$$\gamma_2^2[w_1''(a)-w_{10}''(a)]=\gamma_1^2[w_2''(a)-w_{20}''(a)] \qquad (2.2.5)$$

$$w_1(a)=0,\, w_2(a)=0$$

$$w_2'(a)=w_1'(a)\,.$$

The terms involving w_{10} and w_{20} can be dropped, since w_{10} and w_{20} satisfy the same boundary and transition conditions for $\gamma_1=\beta_1$, $\gamma_2=\beta_2$, and since $\beta_1/\beta_2=\gamma_1/\gamma_2$.

The reaction forces R_2 and R_3 at the supports at x=*a* and x=1, respectively, can be calculated as follows:

$$\bar{R}_2=EI_2[\bar{w}_2'''(\bar{a})-\bar{w}_{20}'''(\bar{a})]-EI_1[\bar{w}_1'''(\bar{a})-\bar{w}_{10}'''(\bar{a})]$$

so that

$$R_2=\frac{\beta_1^2}{\beta_2^2}[w_2'''(a)-w_{20}'''(a)]-[w_1'''(a)-w_{10}'''(a)], \qquad (2.2.6)$$

and

$$\bar{R}_3 = -EI_2[\bar{w}_2'''(L) - \bar{w}_{20}'''(L)] - P\bar{w}_2'(L)$$

so that

$$R_3 = -\frac{\beta_1^2}{\beta_2^2}[w_2'''(1) - w_{20}'''(1)] - \gamma_1^2 w_2'(1). \tag{2.2.7}$$

Equations (2.2.6) and (2.2.7) can be written as

$$\begin{aligned} R_2 = \frac{\beta_1^2}{\beta_2^2}[&-D_1\gamma_2^3 \cos\gamma_2 a + D_2\gamma_2^3 \sin\gamma_2 a - Y\beta_2^3 \cos\beta_2 a \\ &+ Z\beta_2^3 \sin\beta_2 a + \widetilde{B}_1\beta_2^3 \cos\beta_2 a - \widetilde{B}_2\beta_2^3 \sin\beta_2 a] \\ &+ C_1\gamma_1^3 \cos\gamma_1 a + W\beta_1^3 \cos\beta_1 a - \widetilde{A}_1\beta_1^3 \cos\beta_1 a \end{aligned} \tag{2.2.8}$$

and

$$\begin{aligned} R_3 = -\frac{\beta_1^2}{\beta_2^2}[&-D_1\gamma_2^3 \cos\gamma_2 + D_2\gamma_2^3 \sin\gamma_2 - Y\beta_2^3 \cos\beta_2 + Z\beta_2^3 \sin\beta_2 \\ &+ \widetilde{B}_1\beta_2^3 \cos\beta_2 - \widetilde{B}_2\beta_2^3 \sin\beta_2] - \gamma_1^2[D_1\gamma_2 \cos\gamma_2 \\ &- D_2\gamma_2 \sin\gamma_2 + D_3 + Y\beta_2 \cos\beta_2 - Z\beta_2 \sin\beta_2]. \end{aligned} \tag{2.2.9}$$

The coefficients that are used to get the reaction forces and the maximum deflections can be obtained by the following formulas:

$$D_2 = D_1\alpha_1 + \alpha_2$$

$$D_4 = D_3\alpha_3 + \alpha_4$$

$$C_1 = D_1\alpha_5 + \alpha_6$$

and

$$\delta_{11}D_1+\delta_{12}D_3+\delta_{13}C_3=\delta_{14}$$

$$\delta_{21}D_1+\delta_{22}D_3+\delta_{23}C_3=\delta_{24} \qquad (2.2.10)$$

$$\delta_{31}D_1+\delta_{32}D_3+\delta_{33}C_3=\delta_{34}$$

The above simultaneous equations in D_1, D_3, and C_3 are solved by the Gauss elimination method. The coefficients in the above equations are given in the Appendix.

The size of the initial deflection in this case is specified by setting

$$\tilde{A}_1=\frac{1}{1000W_m}$$

where $W_m=\max.(w_{1m}/a, w_{2m}/b)$

w_{1m}=maximum deflection in the span a of the buckling mode for the perfect column when $\tilde{A}_1=1$

w_{2m}=maximum deflection in the span b of the buckling mode for the perfect column when $\tilde{A}_1=1$

Then the size of the initial deflection is such that the maximum ratio of the deflection magnitude to the length of the span in which it occurs is 1/1000. The quantity W_{max} is the largest deflection (in magnitude) of the column. For example, if $a=0.1$, $W_m=\max.(0.007/0.1, 0.677/0.9)=(0.677/0.9)=0.75$ and the maximum deflection W_{max} is $W_{max}=0.9/1000=0.0009$ when p=0. Similarly, other maximum deflections W_{max} when p=0 can be calculated. They are either given by $a/1000$ or $b/1000$. The values of w_{1m} and w_{2m} are presented for different a's in Table 1.2. If the w_{1m} value is underlined, the maximum initial deflection is

W_{max}=*a*/1000. If the w_{2m} value is underlined, which occurs for this case, the maximum initial deflection is W_{max}=*b*/1000.

Figure 2.16 shows the magnitude of the reaction forces R_2 and R_3 for different *a*'s. There are no reaction forces R_2 and R_3 when *a*=0.5 ; even though the applied load p amplifies the magnitude of a sine curve, it has no effect on the reaction forces R_2 and R_3. Results for *a*)0.5 can be obtained by symmetry.

Figure 2.17 shows the maximum deflection W_{max} for different *a*'s. If the intermediate support is close to the support at x=0 or x=1, the maximum deflection W_{max} at a fixed p has higher values than any other intermediate support location in this case. If the initial deflection $w_0(x)=C\sin 2\pi x$, the deflection w(x) when $\gamma_1=\gamma_2\equiv\gamma$ is

$$w(x)=\frac{4\pi^2 C\ \sin 2\pi x}{4\pi^2-\gamma^2} \qquad (2.2.11)$$

When *a*=0.5, C=0.0005 in the above equation, and the maximum deflection W_{max} can be written as follows:

$$W_{max}=\frac{4\pi^2(0.0005)}{4\pi^2-\gamma^2} \qquad (2.2.12)$$

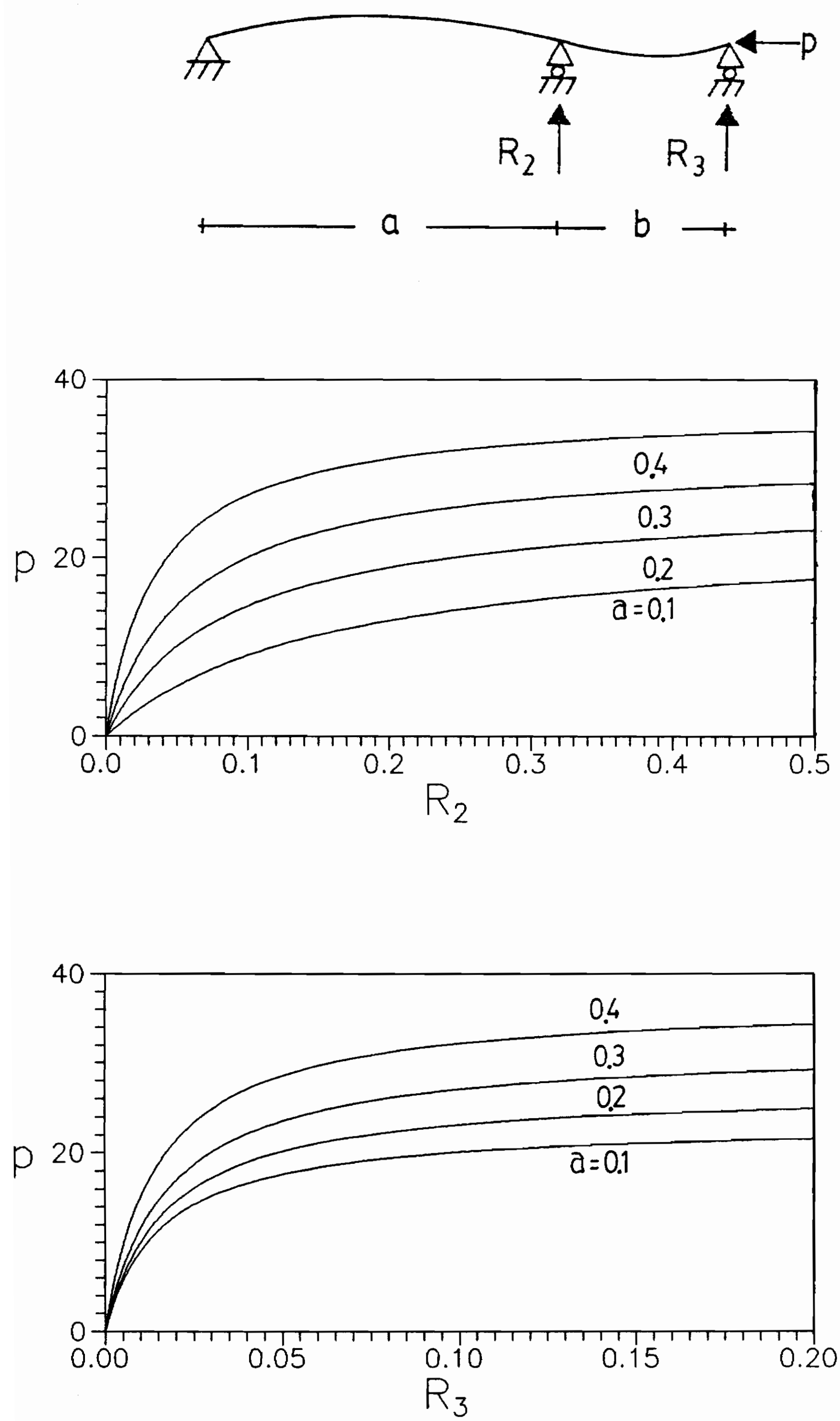

Figure 2.16 Reaction Forces R_2 and R_3 for Different *a*'s

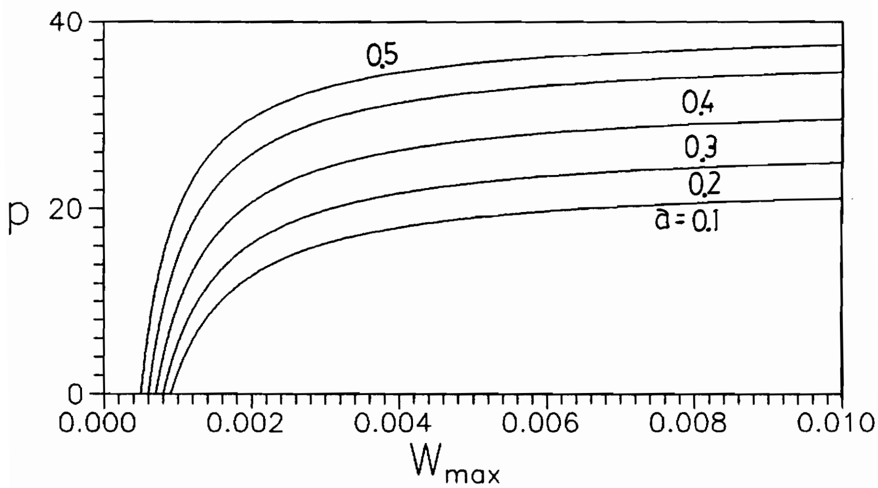

Figure 2.17 **Maximum Deflection W_{max} for Different *a*'s**

b. <u>Case VI : Case II with Initial Deflection</u>

The boundary and transition conditions for this case are

$$w_1(0)=0,w_1''(0)-w_{10}''(0)=0$$

$$w_2(1)=0,w_2''(1)-w_{20}''(1)=0$$

$$w_2(a)=w_1(a),w_2'(a)=w_1'(a)$$

(2.2.13)

$$\gamma_1^2[w_2'''(a)-w_{20}'''(a)]+\gamma_2^2k[w_1(a)-w_{10}(a)]=\gamma_2^2[w_1'''(a)-w_{10}'''(a)]$$

$$\gamma_2^2[w_1''(a)-w_{10}''(a)]=\gamma_1^2[w_2''(a)-w_{20}''(a)]$$

Again the terms involving w_{10} and w_{20} can be dropped.

The reaction forces R_2 and R_3 at x=a and x=1, respectively, can be calculated as follows:

$$\bar{R}_2=\bar{k}[EI_1\bar{w}_1(\bar{a})-EI_1\bar{w}_{10}(\bar{a})]$$

so that

$$R_2=k[w_1(a)-w_{10}(a)]$$

(2.2.14)

and

$$\bar{R}_3=-EI_2[\bar{w}_2'''(L)-\bar{w}_{20}'''(L)]-P\bar{w}_2'(L)$$

so that

$$R_3 = -\frac{\beta_1^2}{\beta_2^2}[w_2'''(1) - w_{20}'''(1)] - \gamma_1^2 w_2'(1) \tag{2.2.15}$$

Equation (2.2.14) can be written as

$$R_2 = k[C_1 \sin\gamma_1 a + C_3 a + W\sin\beta_1 a - \tilde{A}_1 \sin\beta_1 a - \tilde{A}_3 a] \tag{2.2.16}$$

and Equation (2.2.15) is the same as Equation (2.2.9).

The formulas for all the coefficients that are used to get the reaction forces and the maximum deflections are the same as for Case V. However, the variables used in each formula are not the same as before. All the variables are given in the Appendix.

In order to get the maximum deflections for different *a*'s, $\tilde{A}_1$ is set as

$$\tilde{A}_1 = \frac{1}{1000 W_m}$$

where $W_m = \max.(w_{1m}, w_{2m})$

w_{1m} = maximum deflection in the span *a* of the buckling mode for the perfect column when $\tilde{A}_1 = 1$

w_{2m} = maximum deflection in the span *b* of the buckling mode for the perfect column when $\tilde{A}_1 = 1$

Then the maximum initial deflection is 1/1000 of the length of the column for this case. Table 2.3 shows the values of w_{1m} and w_{2m} for different *a*'s with k=50. From Table 2.3, the values of W_m can be obtained. For example, if *a*=0.1, W_m=max.(0.553,1.881)=1.881 and W_{max} when p=0 is 1/1000. Table 2.4 shows the values of w_{1m} and w_{2m} for different *a*'s with k=200. In this case, the values of W_m are W_m=3.727, 3.135, 3.796, 3.695, and 1.0 for *a*=0.1, 0.2, 0.3, 0.4, and 0.5, respectively, and W_{max} when p=0 is always 1/1000.

Figure 2.18 shows the magnitude of the reaction forces R_2 and R_3 for different *a*'s with k=50, and Figure 2.19 shows the reaction forces R_2 and R_3 for different *a*'s with k=200. Note that the scale on the R_2 axis is ten times larger than the scale on the R_3 axis in Figure 2.19. As the applied load p increases, the magnitudes of the reaction forces R_2 and R_3 when k=200 have higher values than those of the reaction forces R_2 and R_3 when k=50. If $a=0.5$ and $k>16\pi^2$, there are no reaction forces R_2 and R_3. In this case, the applied load p has no effect on the reaction forces R_2 and R_3. Results for $a>0.5$ can be obtained by symmetry.

Figure 2.20 and Figure 2.21 show the maximum deflections for different *a*'s with k=50 and k=200, respectively. If $a=0.5$ and $k>16\pi^2$, Equation (2.2.11) can be used to get the maximum deflection for this case.

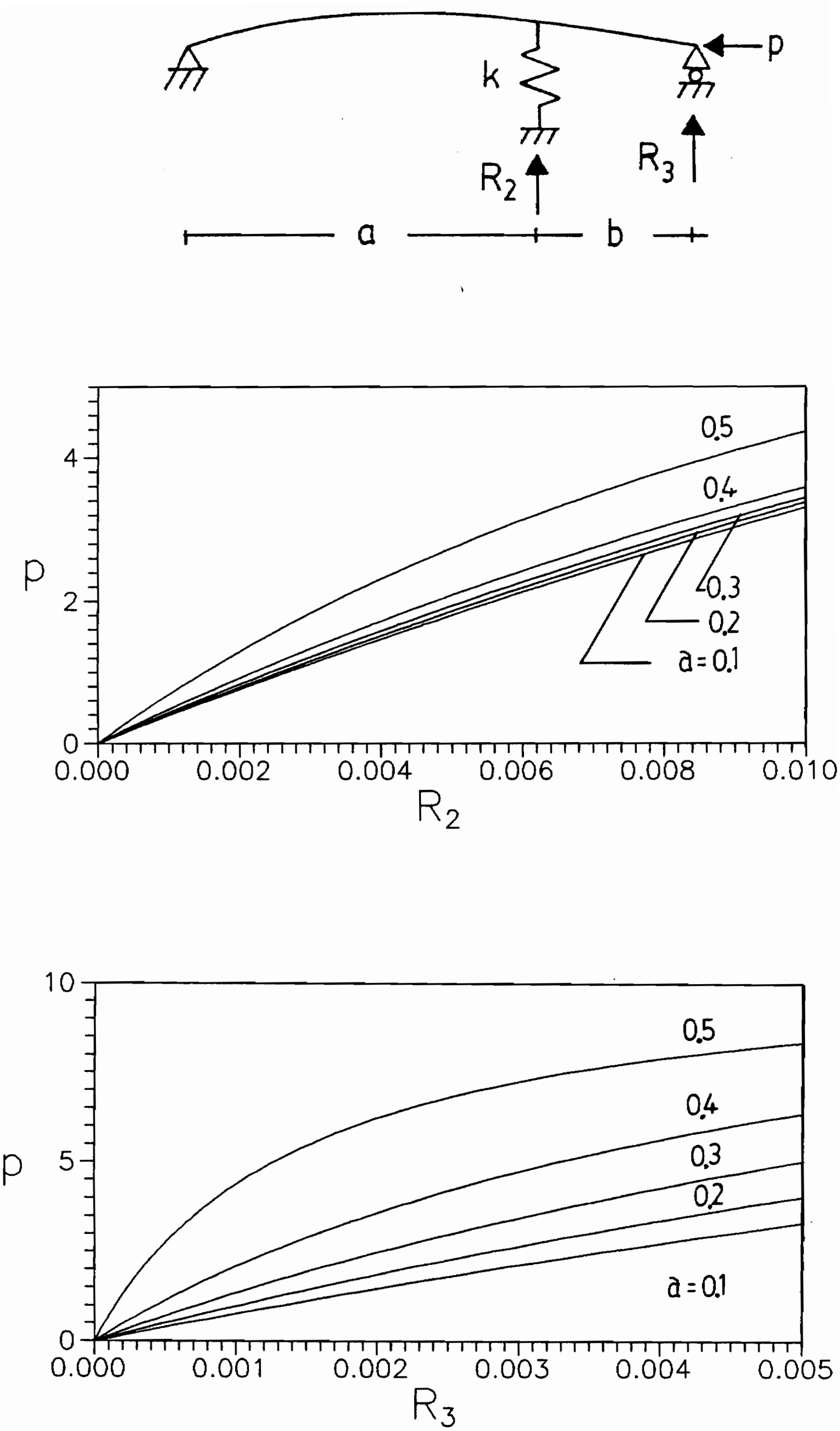

Figure 2.18 Reaction Forces R_2 and R_3 for Different *a*'s with k=50

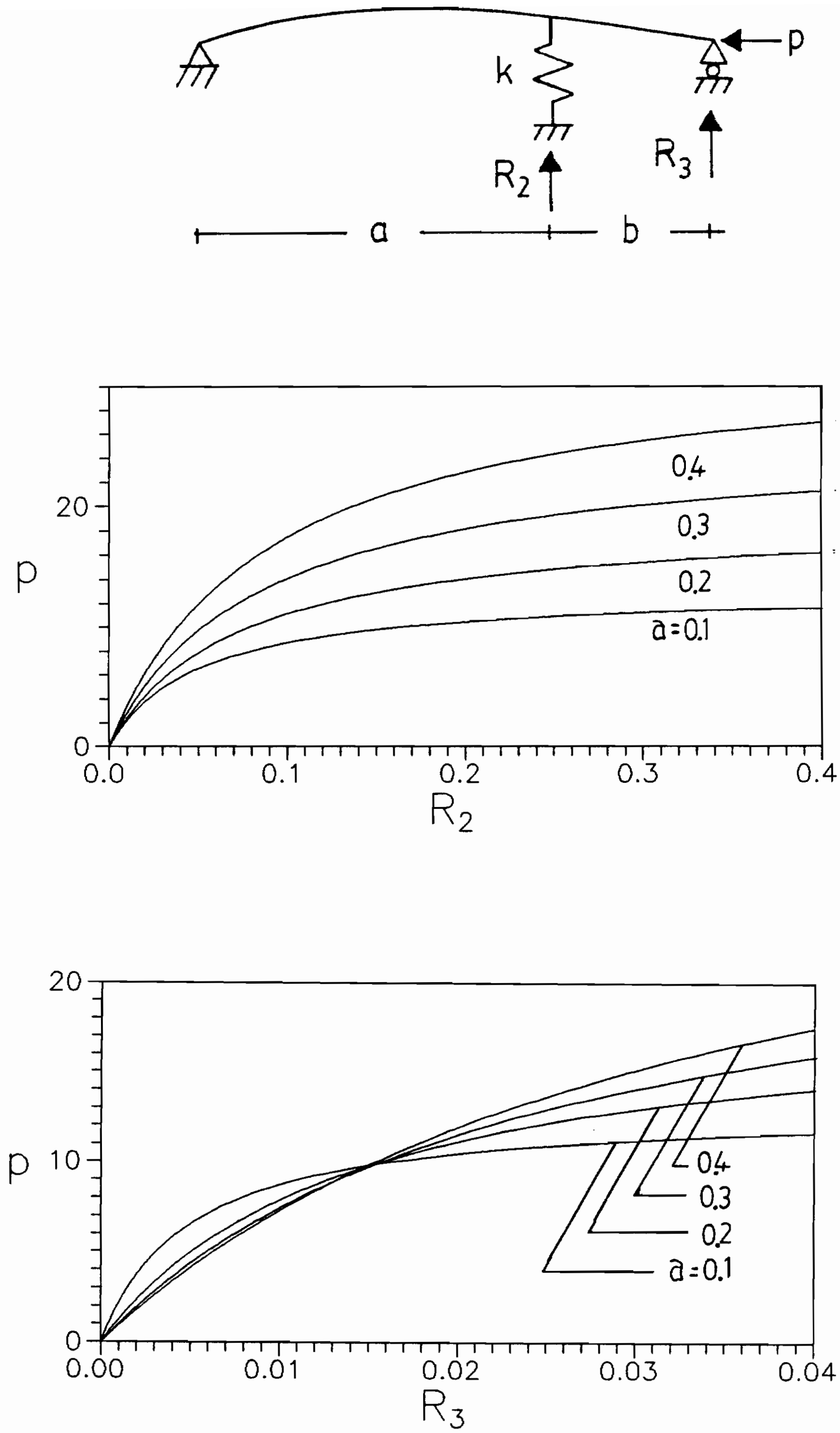

Figure 2.19 Reaction Forces R_2 and R_3 for Different *a*'s with k=200

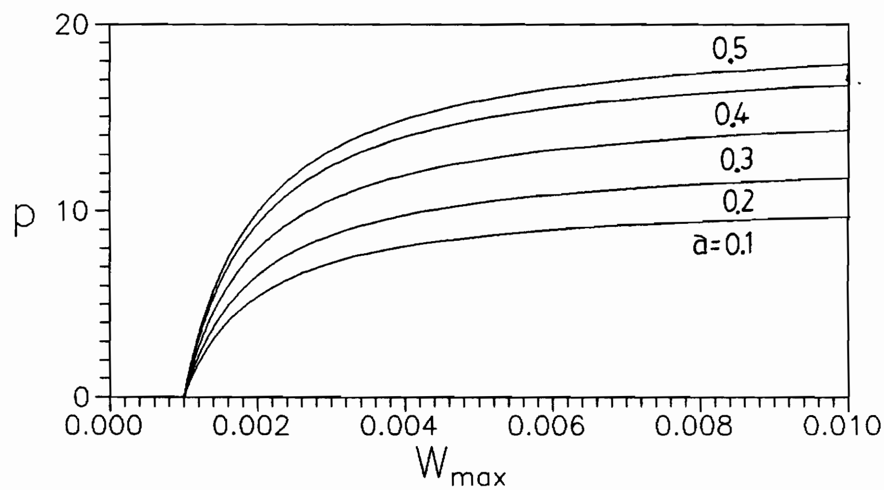

Figure 2.20 Maximum Deflection W_{max} for Different *a*'s with k=50

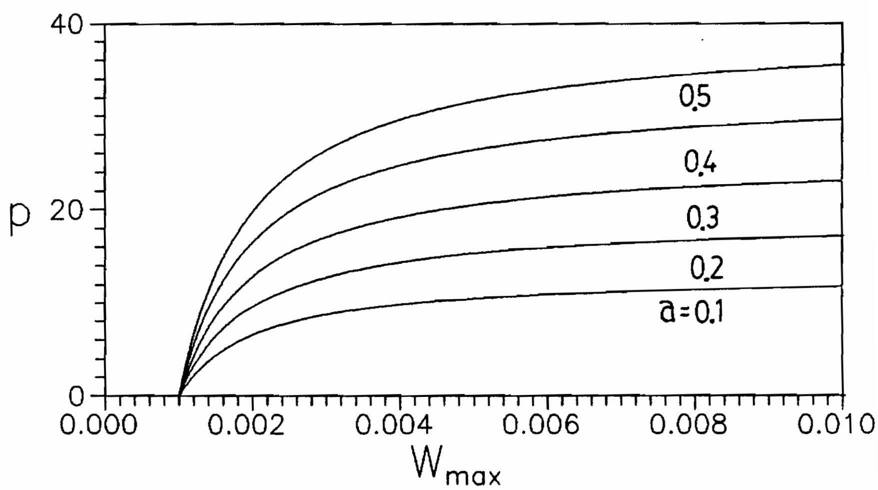

Figure 2.21 Maximum Deflection W_{max} for Different a's with k=200

c. <u>Case VII : Case III with Initial Deflection</u>

The boundary and transition conditions for this case are

$$w_1(0)=0,\, w_1''(0)-w_{10}''(0)=0$$

$$w_2''(1)-w_{20}''(1)=0$$

$$\gamma_1^2[w_2'''(1)-w_{20}'''(1)]+\gamma_1^2\gamma_2^2 w_2'(1)=\gamma_2^2 k_2[w_2(1)-w_{20}(1)]$$

$$w_1(a)=w_2(a),\, w_1'(a)=w_2'(a) \qquad (2.2.17)$$

$$\gamma_2^2[w_1''(a)-w_{10}''(a)]=\gamma_1^2[w_2''(a)-w_{20}''(a)]$$

$$\gamma_1^2[w_2'''(a)-w_{20}'''(a)]+\gamma_2^2 k_1[w_1(a)-w_{10}(a)]=\gamma_2^2[w_1'''(a)-w_{10}'''(a)]$$

The w_{10} and w_{20} terms in the shear force condition at x=1 (involving k_2) do not cancel each other.

The reaction forces R_2 and R_3 for each support can be calculated as follows:

$$R_2=\bar{k}_1[EI_1\bar{w}_1(\bar{a})-EI_1\bar{w}_{10}(\bar{a})]$$

so that

$$R_2=k_1[w_1(a)-w_{10}(a)]$$

(2.2.18)

and

$$\bar{R}_3 = k_2[EI_2\bar{w}_2(L) - EI_2\bar{w}_{20}(L)]$$

so that

$$R_3 = k_2[w_2(1) - w_{20}(1)] \tag{2.2.19}$$

Equations (2.2.18) and (2.2.19) can be written as

$$R_2 = k_1[C_1\sin\gamma_1 a + C_3 a + W\sin\beta_1 a - \tilde{A}_1\sin\beta_1 a - \tilde{A}_3 a] \tag{2.2.20}$$

and

$$R_3 = k_2[D_1\sin\gamma_2 + D_2\cos\gamma_2 + D_3 + D_4 + Y\sin\beta_2 + Z\cos\beta_2 - \tilde{B}_1\sin\beta_2 - \tilde{B}_2\cos\beta_2 - \tilde{B}_3 - \tilde{B}_4] \tag{2.2.21}$$

The formulas of all the coefficients that are used to get the reaction forces and the maximum deflections can be obtained as follows:

$$D_2 = D_1\alpha_1 + \alpha_2$$

$$D_4 = D_1G_6 + D_3G_7 + G_8$$

$$C_1 = D_1\alpha_5 + \alpha_6$$

and

$$\delta_{11}D_1 + \delta_{12}D_3 + \delta_{13}C_3 = \delta_{14}$$

$$\delta_{21}D_1 + \delta_{22}D_3 + \delta_{23}C_3 = \delta_{24} \tag{2.2.22}$$

$$\delta_{31}D_1+\delta_{32}D_3+\delta_{33}C_3=\delta_{34}$$

All the variables that are used in the above equations are given in the Appendix.

In order to get the maximum deflection for different a's, $\tilde{A}_1$ is specified as before for Case VI. Table 3.3 shows the values of w_{1m} and w_{2m} for different a's with k=50. By using these values of w_{1m} and w_{2m}, the maximum deflections W_{max} when p=0 are obtained. In this case, the values of W_m are W_m=max.(w_{1m},w_{2m})=w_{2m}=1.830, 2.804, 2.738, and 1.953 for a=0.1, 0.2, 0.3, and 0.4, respectively, and W_m=max.(w_{1m},w_{2m})=w_{1m}=1.386, 1.148, 1.035, 0.970, and 0.951 for a=0.5, 0.6, 0.7, 0.8, and 0.9, respectively. The maximum deflections W_{max} when p=0 are always 1/1000 in this case. Table 3.4 and Table 3.5 show the values of w_{1m} and w_{2m} for different a's with k=200 and k=300, respectively.

Figure 2.22 and Figure 2.23 show the magnitude of the reaction forces R_2 and R_3 for different a's with k=50. Figure 2.24 and Figure 2.25 show the reaction forces R_2 and R_3 for different a's with k=200. Figure 2.26 and Figure 2.27 show the reaction forces R_2 and R_3 for different a's with k=300. As the applied load p increases, the magnitudes of the reaction forces R_2 and R_3 when k=200 have higher values than those of the reaction forces R_2 and R_3 when k=50. However, the magnitudes of the reaction forces R_2 and R_3 when k=300 are often smaller than those of the reaction forces R_2 and R_3 when k=200. If a=0.5 and k⟩206.7117, there are no reaction forces R_2 and R_3.

Figure 2.28 and Figure 2.29 show the maximum deflection W_{max} for k=50 and k=200, respectively. As the applied load p increases, the magnitudes of the maximum deflections W_{max} increase. Figure 2.30 shows the maximum deflection for different a's with k=300. If a=0.5 and k⟩206.7117, the following coefficients are used to get the maximum deflections:

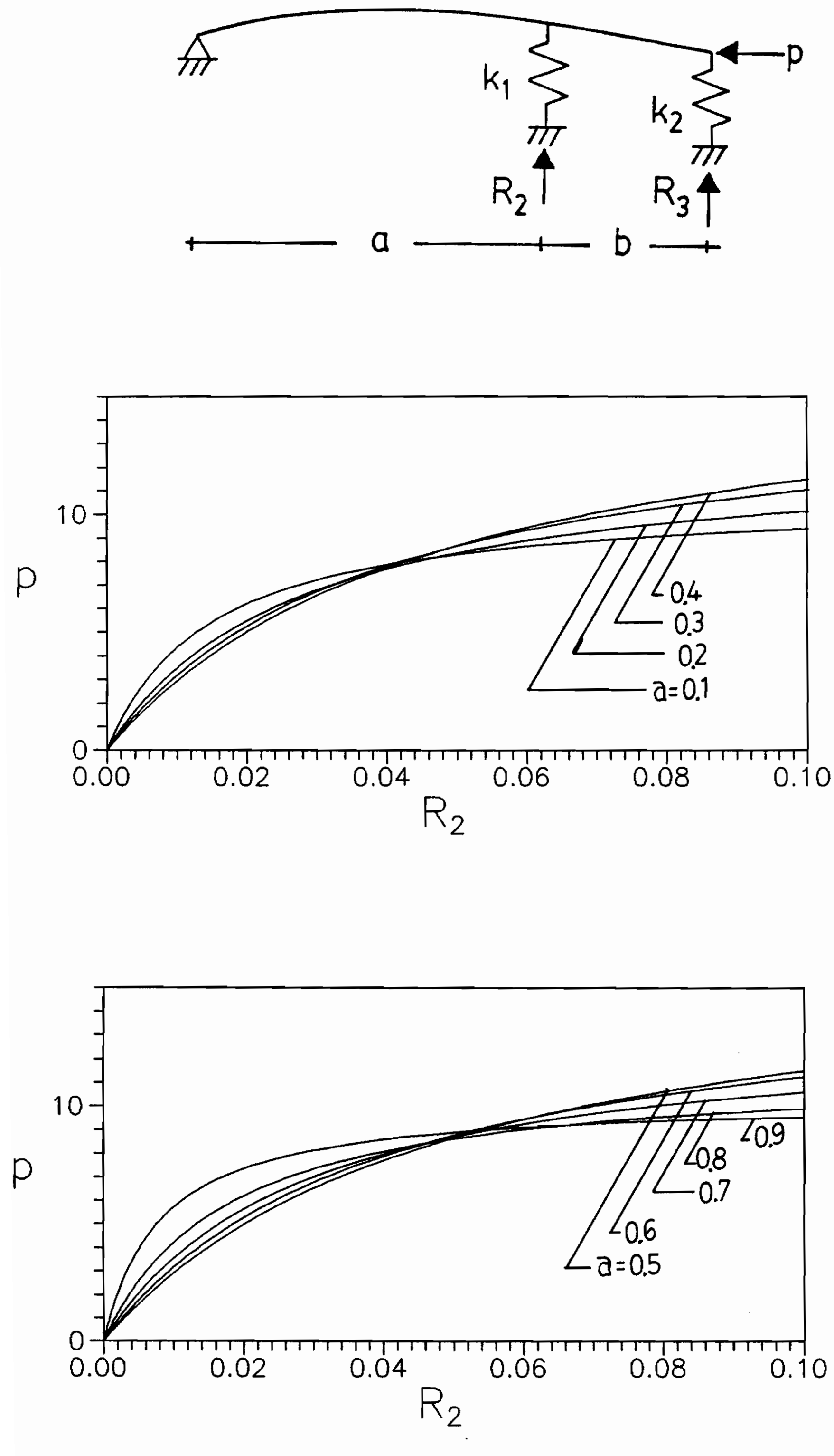

Figure 2.22 Reaction Force R_2 for Different *a*'s with k=50

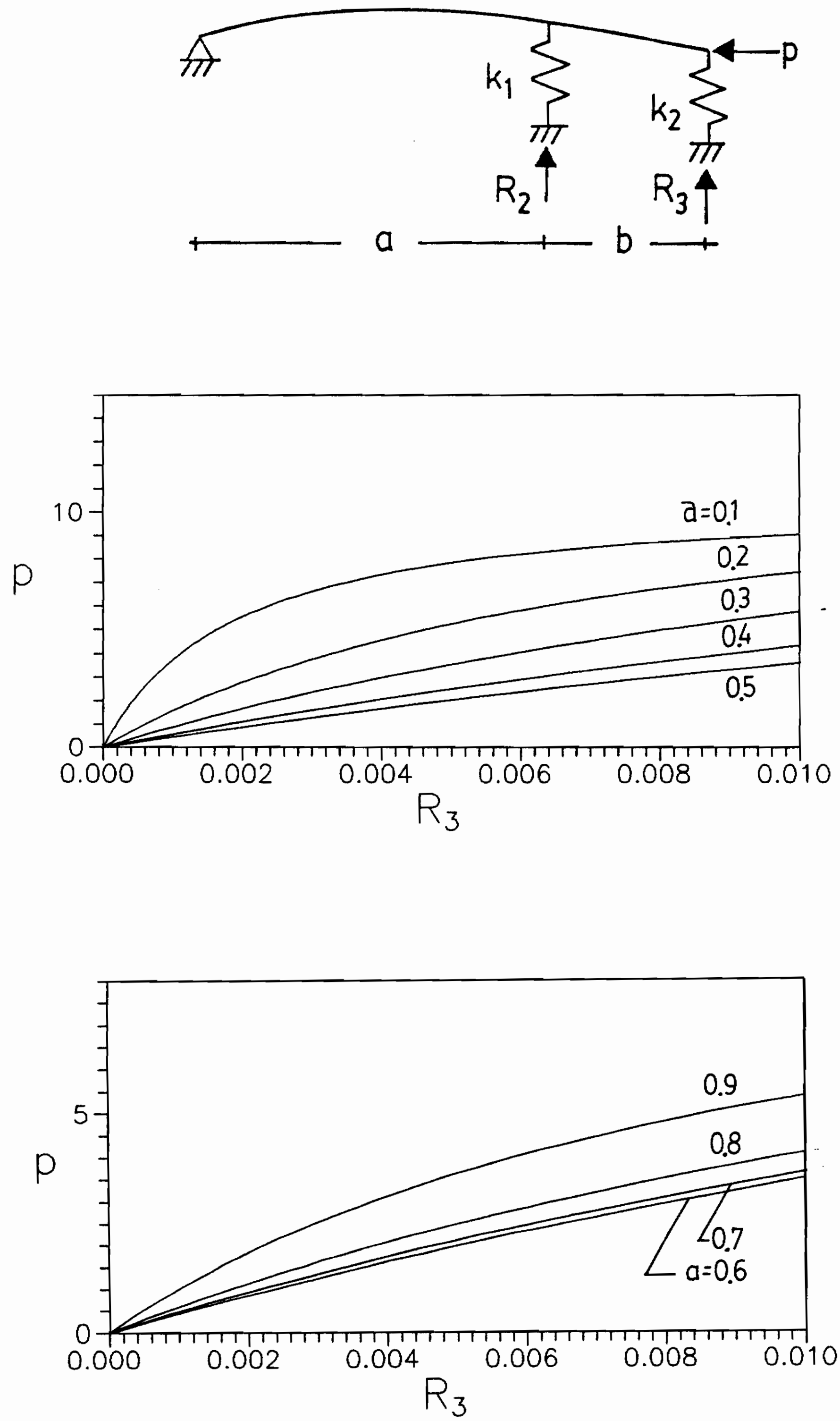

Figure 2.23 Reaction Force R_3 for Different *a*'s with k=50

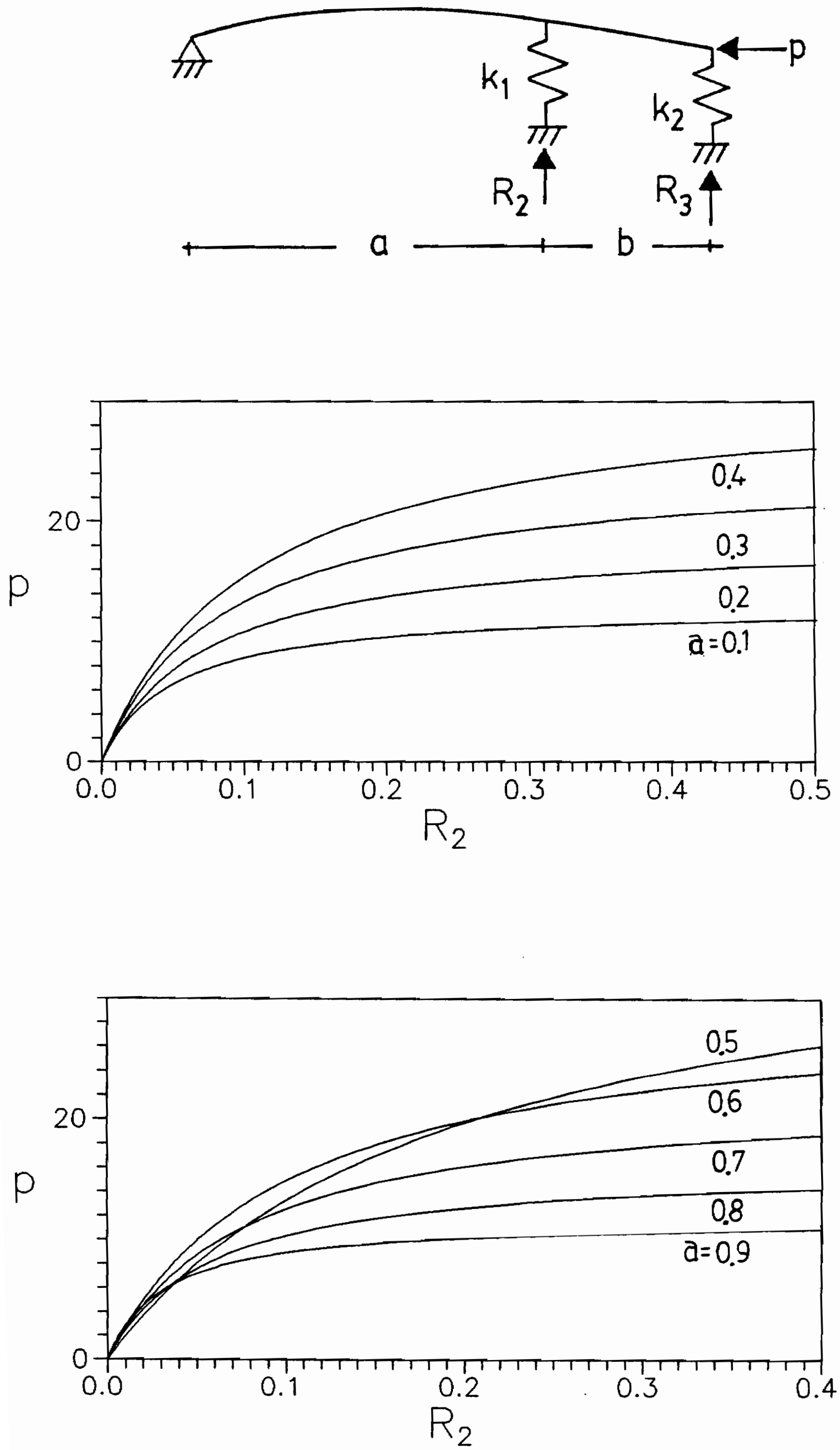

Figure 2.24 **Reaction Force R_2 for Different *a*'s with k=200**

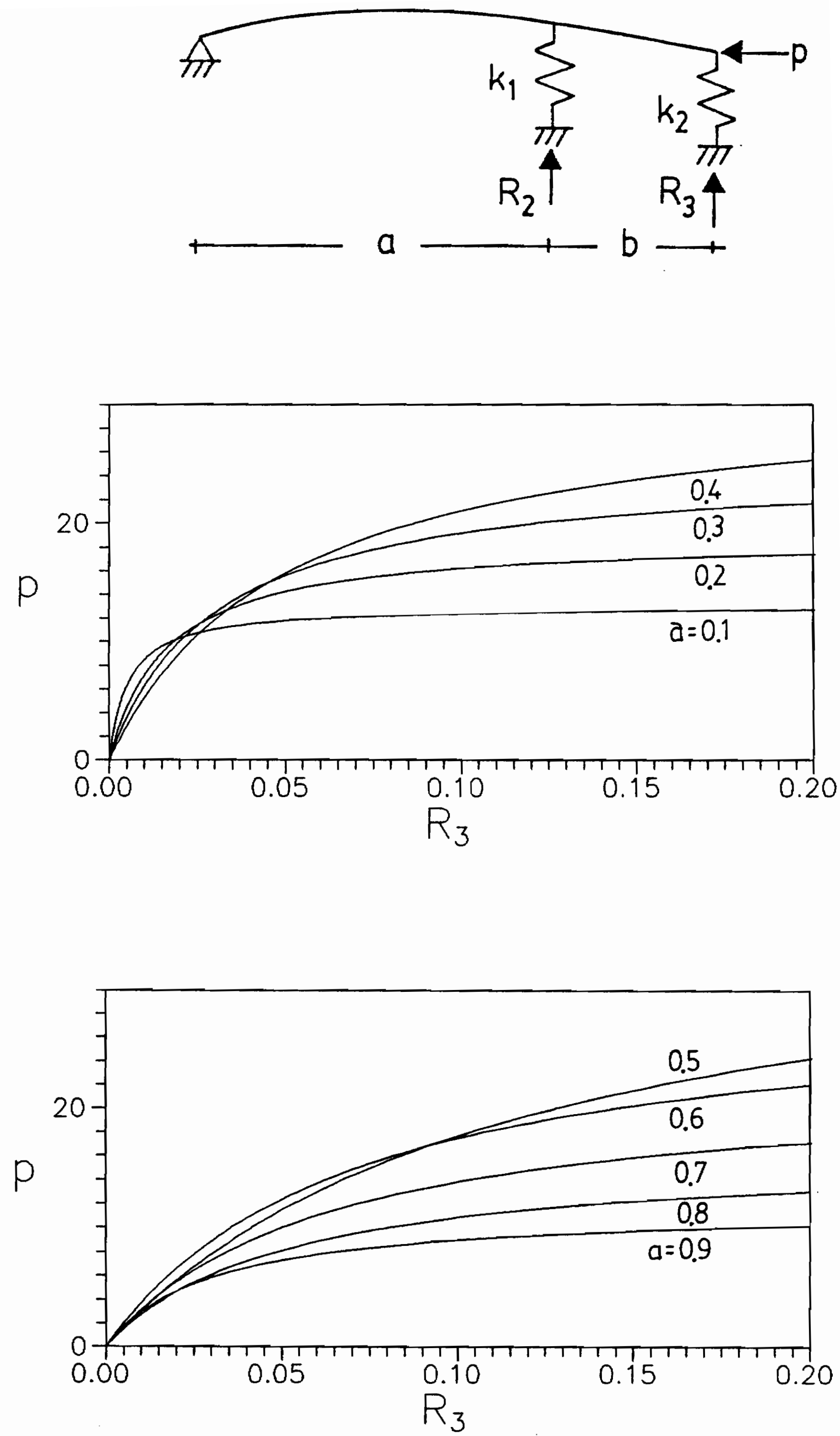

Figure 2.25 Reaction Force R_3 for Different *a*'s with k=200

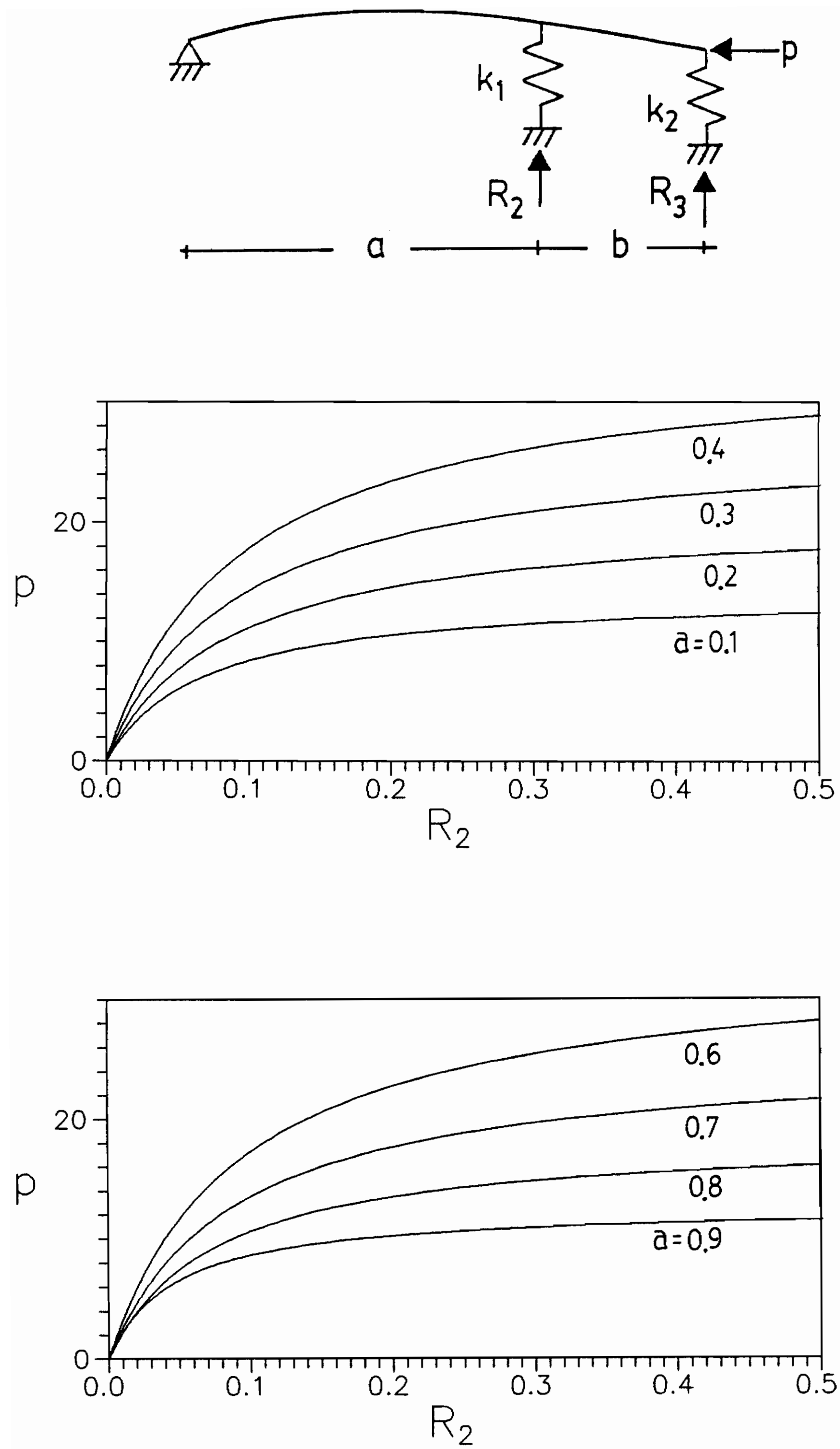

Figure 2.26 Reaction Force R_2 for Different *a*'s with k=300

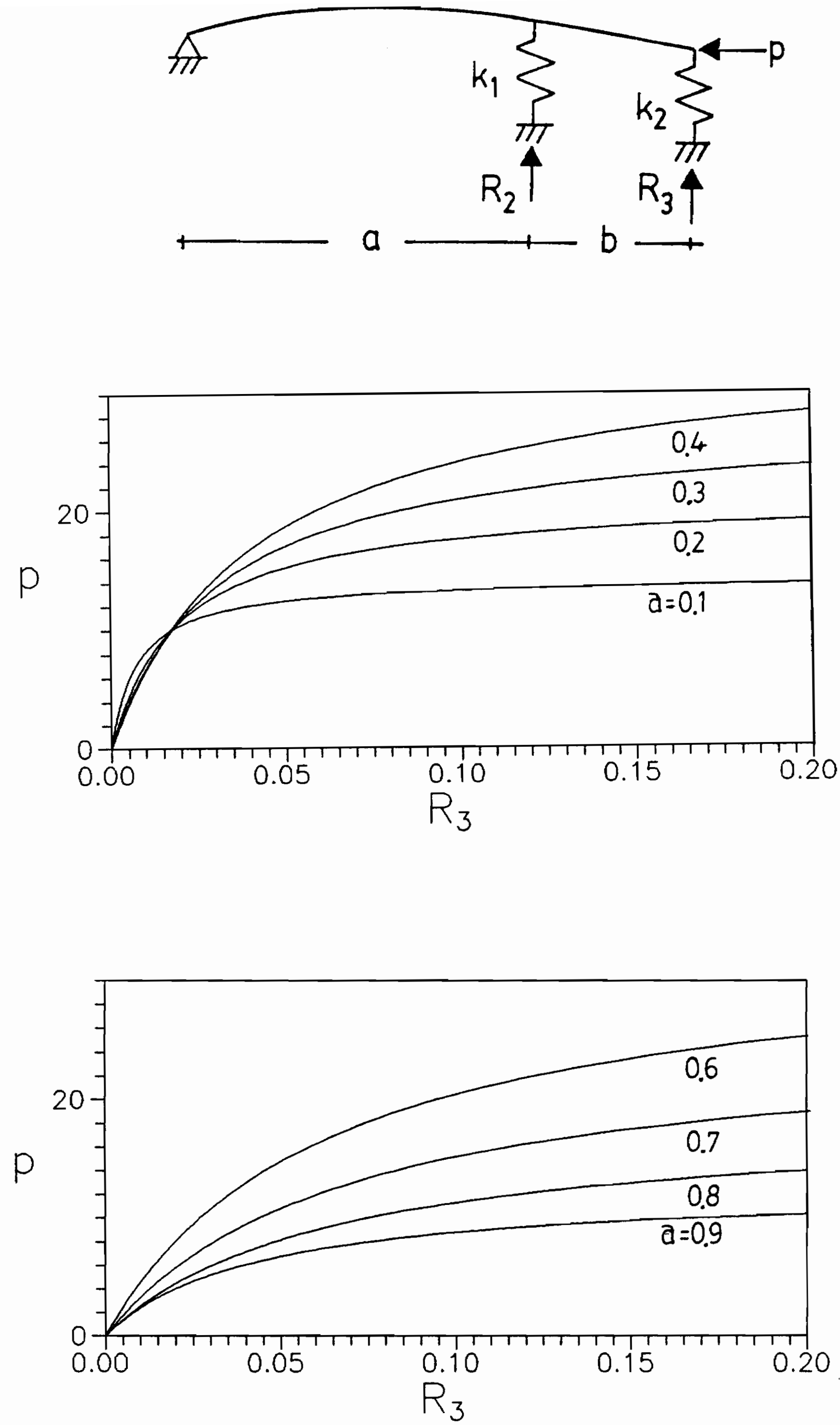

Figure 2.27 **Reaction Force R_3 for Different *a*'s with k=300**

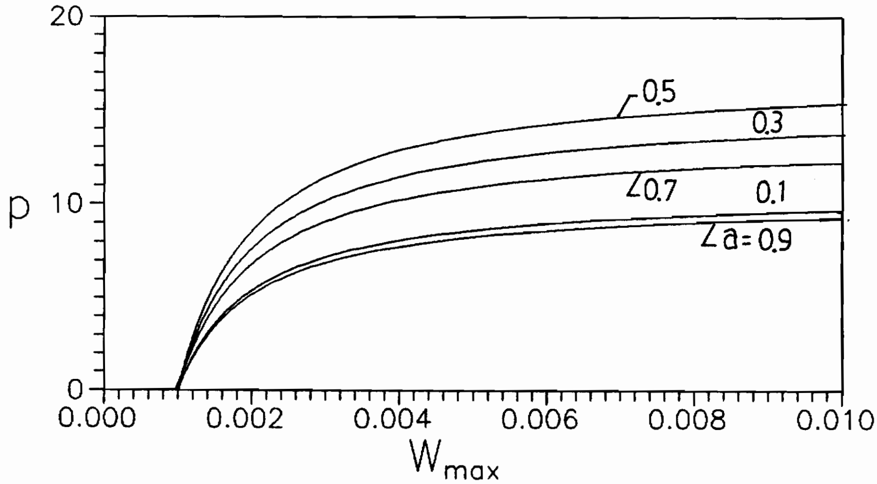

Figure 2.28 Maximum Deflection W_{max} for Different a's with k=50

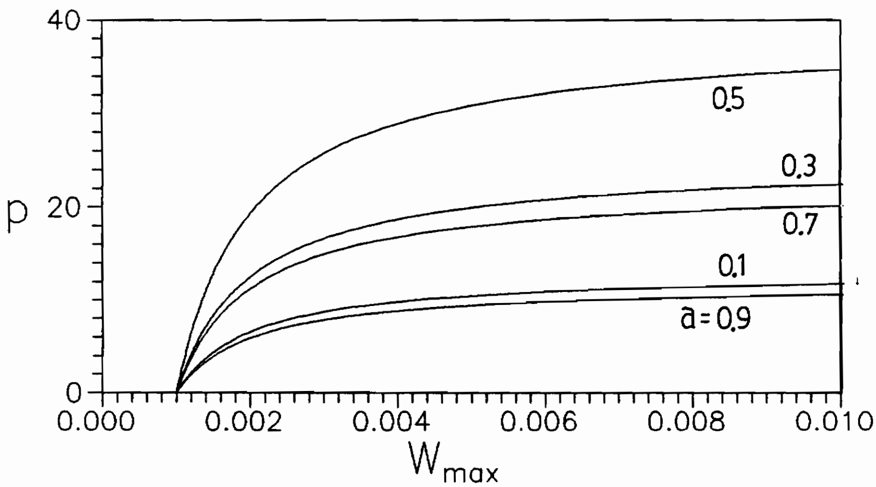

Figure 2.29 Maximum Deflection W_{max} for Different *a*'s with k=200

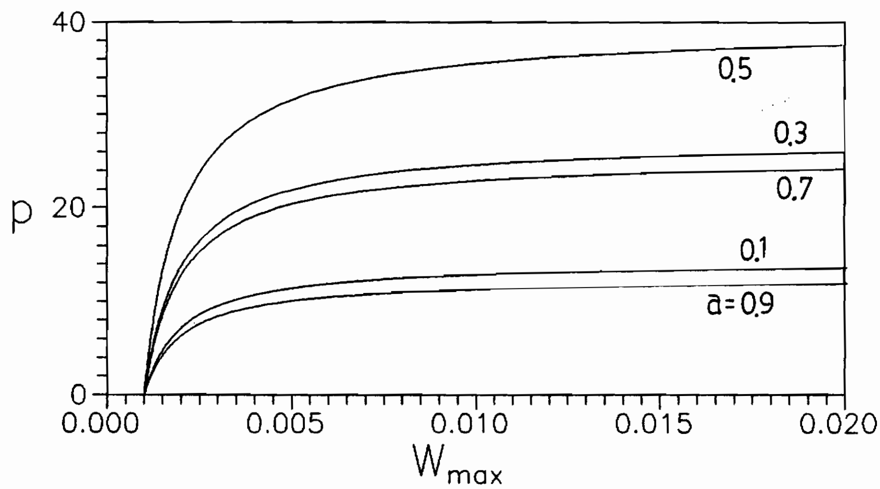

Figure 2.30 Maximum Deflection W_{max} for Different a's with k=300

$$\widetilde{A}_1 = \frac{1}{1000 W_m}$$

$$\widetilde{B}_1 = \widetilde{A}_1$$

$$\widetilde{A}_3 = \widetilde{B}_2 = \widetilde{B}_3 = \widetilde{B}_4 = 0$$

CHAPTER 3

SUMMARY AND CONCLUSIONS

3.1 Perfect Columns

Four perfect two-span columns subjected to an axial compressive load P were investigated first. Each column was allowed to have different bending stiffnesses EI_i, (i=1,2), in each span, in the general formulation, but all numerical results were obtained for uniform columns ($EI_1=EI_2$). The columns under consideration were shown in Figure 2.1. In the numerical results, k_1 and k_2 were assumed to be equal.

In each case, the investigation was carried out to find the critical load P_{cr} as a function of the span lengths and to show the effects of the rotational spring stiffness c and the translational spring stiffnesses k_1 and k_2 on the critical load P_{cr} for different span lengths. In addition, conditions for the existence of an ideal spring stiffness were also examined.

The results discussed in section 2.1 apply to a uniform column ($EI_1=EI_2$) and can be summarized as follows:

1. If an intermediate support is located in the middle of a pinned-pinned column (a=0.5), the column can resist a higher applied load P than for any other support location in Case I.

   If an intermediate translational spring k is located in the middle of a pinned-pinned column (a=0.5), the column can resist a higher applied load P than for any other spring location in Case II.

   For Case III, the optimal location of the intermediate translational spring k is not located in the middle of the two-span column. It depends on the translational spring stiffnesses k ($k_1=k_2\equiv k$) at $x=a$ and $x=1$.

2. The ideal spring stiffness k_{ideal} exists only for a=0.5 in Case II and Case III if $EI_1=EI_2$. The values are $k_{ideal}=16\pi^2$ and k_{ideal}=206.7117 for Case II and Case III, respectively. If $k \geq k_{ideal}$, the critical load is $p_{cr}=4\pi^2$ when a=0.5 in both of these cases.

   In Case IV, there are no values k_{ideal} for fixed values of c and a and no c_{ideal} for fixed values of k ($k_1=k_2\equiv k_3$) and a.

3. The curves in Figure 2.10 and Figure 2.11 are not symmetric about a=0.5. In Figure 2.10, if c=0, the result is exactly the same for k=200 as shown in Figure 2.8 for Case III. If $c \to \infty$, the end x=0 is a fixed end and the critical load p_{cr}=43.521 for $a \approx 0.6$ when $k_1=k_2=200$ is the highest p_{cr}.

4. If a=0.5, the buckling mode shape is a sine curve for Case I. If a=0.5 and $k \geq k_{ideal}$, the buckling mode shape is also a sine curve for Case II and Case III ($k_1=k_2\equiv k$).

3.2 Imperfect Columns

Three imperfect columns subjected to an axial compressive load P were investigated. Each column was allowed to have different bending stiffnesses EI_i, (i=1,2), in each span. The initial deflections of each column have the shape of the buckling mode of the corresponding perfect column and have a specified size. The columns under consideration were shown in Figure 2.1 (a)-(c). Cases V, VI, and VII correspond to Case I, II, and III, respectively, with initial curvature. In each case, the investigation was carried out to find the reaction forces R_2 and R_3 at x=a and x=L, respectively, and to find the maximum deflection of each column, as functions of the applied load P.

The results discussed in section 2.2 apply to the case of a uniform column ($EI_1=EI_2$) and can be summarized as follows:

1. In Case V, there are no reaction forces R_2 and R_3 when a=0.5; even though the applied load p amplifies the magnitude of a sine curve, it has no effect on the reaction forces R_2 and R_3.

   The above result is the same for Case VI and Case VII if a=0.5 and $k>k_{ideal}$ for each case, respectively.
2. In Case V, if the intermediate support is close to the support at x=0 or x=1, the maximum deflections W_{max} at a fixed P show higher values than for any other intermediate support location.

   In Case VI and Case VII, if the intermediate translational spring is close to the support at x=0 or to the translational spring at x=1, the maximum deflections W_{max} show higher values than for any other intermediate translational spring location.
3. Reaction forces and maximum deflections are proportional to the size of the initial deflection. Their values for initial deflections of the same shape but different size can be determined directly from the results presented here.
4. The shape of the initial deflection chosen here was that of the buckling mode of the corresponding perfect column. Under compression, this shape tends to lead to larger deflections than other initial deflections having the same size (e.g., the same maximum initial deflection).

3.3 Recommendations for Future Work

Some recommendations for future study are noted as follows:

1. Investigate other types of laterally braced columns with various load conditions such as uniformly distributed load or additional axial loads at the internal bracing points.
2. Investigate other types of laterally braced columns with various boundary

conditions such as clamped ends.

3. Investigate braced multiple-span columns with varying span lengths.
4. Investigate two-span columns with unequal spring stiffnesses or unequal moments of inertia in the spans.
5. Investigate the continuous lateral bracing of two-span columns subjected to an axial compressive load.
6. Use other methods such as the Newton-Raphson method or secant method along with the bisection method to improve the efficiency of finding a root for the critical load or the ideal spring stiffness.

REFERENCES

1. Winter, G., "Lateral Bracing of Columns and Beams," Transactions, ASCE, Vol. 125, Part I, 1960, pp. 807-845.

2. Galambos, T. V., Guide to Stability Design Criteria for Metal Structures, John Wiley & Sons, New York, 1988, Fourth Edition, pp. 55-57.

3. Salmon, C. G. and Johnson, J. E., Steel Structures, Harper & Row, New York, 1990, Third Edition, pp. 579-584.

4. McGuire, W., Steel Structures, Prentice-Hall, Englewood Cliffs, New Jersey, 1968, pp. 562-574

5. Zuk, W., "Lateral Bracing Forces on Beams and Columns," Journal of the Engineering Mechanics Divison, ASCE, Vol. 82, EM3, 1956, pp. 1032-1 to 1032-16.

6. Medland, I. C., "A Basis for the Design of Column Bracing," The Structural Engineer, London, England, Vol. 55, No. 7, 1977, pp. 301-307.

7. Medland, I. C. and Segedin, C. M., "Brace Forces in Interbraced Column Structures," Journal of the Structural Division, ASCE, Vol. 105, ST7, 1979, pp. 1543-1556.

8. Beliveau, J.- G. and Zhang, H.- Y., "Minimum Required Lateral Stiffness of Structures," in Mechanics Computing in 1990's and Beyond, H. Adeli and R. L. Sierakowski, editors, ASCE, Vol. 1, 1991, pp. 223-227.

9. Plaut, R. H., "Column Buckling When Support Stiffens Under Compression," Journal of Applied Mechanics, Vol. 56, 1989, p. 484.

APPENDIX A

NOTATION

$\bar{a}$ = length of first span

a = nondimensional span length = $\bar{a}/L$

$\tilde{A}_j$ = coefficients of initial deflection in first span

A_j = coefficients of deflection in first span

$\bar{b}$ = length of second span

b = nondimensional span length = $\bar{b}/L$

$\tilde{B}_j$ = coefficients of initial deflection in second span

B_j = coefficients of deflection in second span

β_1 = nondimensional critical load of perfect column = $\sqrt{PL^2/EI_1}$

β_2 = nondimensional critical load of perfect column = $\sqrt{PL^2/EI_2}$

$\bar{c}$ = rotational spring stiffness at $\bar{x}=0$

c = nondimensional rotational spring stiffness at x=0 = $\bar{c}L/EI_1$

c_{ideal} = ideal nondimensional rotational spring stiffness

C_j = coefficients

D_j = coefficients

EI_1 = bending stiffness of first span

EI_2 = bending stiffness of second span

g = stiffening rate of rotational spring

γ_1 = nondimensional load = $\sqrt{PL^2/EI_1}$

γ_2 = nondimensional load = $\sqrt{PL^2/EI_2}$

H_j = coefficients

$\bar{k}$ = intermediate translational spring stiffness at $\bar{x}=\bar{a}$

k = nondimensional intermediate translational spring stiffness at $x=a$ = $\bar{k}L^3/EI_1$

$\bar{k}_1$ = intermediate translational spring stiffness at $\bar{x}=\bar{a}$

k_1 = nondimensional intermediate translational spring stiffness at $x=a$ = $\bar{k}_1L^3/EI_1$

$\bar{k}_2$ = lateral bracing support stiffness at $\bar{x}=\bar{a}+\bar{b}= L$

k_2 = nondimensional lateral bracing support stiffness at $x=1$ = $\bar{k}_2L^3/EI_1$

k_{ideal} = ideal nondimensional translational spring stiffness

p = nondimensional applied axial compressive load = PL^2/EI_1

p_{cr} = nondimensional critical load

P = applied axial compressive load

$\bar{R}_2$ = reaction force at $\bar{x}=\bar{a}$

R_2 = nondimensional reaction force at $x=a$ = $\bar{R}_2L^2/EI_1$

$\bar{R}_3$ = reaction force at $\bar{x}=L$

R_3 = nondimensional reaction force at $x=1$ = $\bar{R}_3L^2/EI_1$

$\bar{w}_1(\bar{x})$ = transverse deflection for $0\le\bar{x}\le\bar{a}$

$w_1(x)$ = nondimensional transverse deflection for $0\le x\le a$ = $\bar{w}_1/L$

$\bar{w}_{10}(\bar{x})$ = initial deflection of the imperfect column for $0\le\bar{x}\le\bar{a}$

$w_{10}(x)$ = nondimensional initial deflection of the imperfect column for $0\le x\le a$ = $\bar{w}_{10}/L$

$\bar{w}_2(\bar{x})$ = transverse deflection for $\bar{a}\le\bar{x}\le L$

$w_2(x)$ = nondimensional transverse deflection for $a\le x\le 1$ = $\bar{w}_2/L$

$\bar{w}_{20}(\bar{x})$ = initial deflection of the imperfect column for $\bar{a}\le\bar{x}\le L$

$w_{20}(x)$ = nondimensional initial deflection of the imperfect column for $a\le x\le 1$ = $\bar{w}_{20}/L$

w_{1m} = maximum nondimensional deflection in the first span of the buckling mode for the perfect column when $\tilde{A}_1=1$

w_{2m} = maximum nondimensional deflection in the second span of the buckling mode for the perfect column when $\tilde{A}_1=1$

W_m = max.$(w_{1m}/a\ ,\ w_{2m}/b)$

W_{max} = maximum deflection of imperfect column

APPENDIX B

Variables Used in Case IV

$$H_1=-\tan\gamma_1 a$$

$$H_2=-\frac{\sin\gamma_2 b}{\cos\gamma_1 a\ \cos\gamma_2}$$

$$H_3=\tan\gamma_1 a$$

$$H_4=\frac{\sin\gamma_2 b}{\cos\gamma_1 a\ \cos\gamma_2}$$

$$H_5=\frac{\gamma_1^2}{c}\ \tan\gamma_1 a-\gamma_1$$

$$H_6=\frac{\gamma_1^2\ \sin\gamma_2 b}{c\ \cos\gamma_1 a\ \cos\gamma_2}$$

$$H_7=-\tan\gamma_2$$

$$H_8=\gamma_1\ \cos\gamma_1 a-H_1\gamma_1\ \sin\gamma_1 a+H_5$$

$$H_9=H_6-H_2\gamma_1\ \sin\gamma_1 a-\frac{\gamma_2\ \cos\gamma_2 b}{\cos\gamma_2}$$

$$H_{10}=H_8\left(\frac{\gamma_1^2}{k_2}-1\right)$$

$$H_{11}=H_9\left(\frac{\gamma_1^2}{k_2}-1\right)$$

$$H_{12}=\sin\gamma_1 a+H_1\cos\gamma_1 a+H_5 a+H_3-H_8 a-H_{10}$$

$$H_{13}=\sin\gamma_2 a+H_7\cos\gamma_2 a+H_9 a+H_{11}-H_2\cos\gamma_1 a-H_6 a-H_4$$

$$H_{14}=\frac{H_{12}}{H_{13}}$$

$$H_{15}=-\gamma_1^3\cos\gamma_1 a-k_1\sin\gamma_1 a$$

$$H_{16}=\gamma_1^3\sin\gamma_1 a-k_1\cos\gamma_1 a$$

APPENDIX C

Variables Used in Case V

$$\alpha_1 = -\tan\gamma_2$$

$$\alpha_2 = -\frac{\beta_2^2}{\gamma_2^2 \cos\gamma_2}(Y \sin\beta_2 + Z \cos\beta_2)$$

$$\alpha_3 = -1$$

$$\alpha_4 = \left(\frac{\beta_2^2 - \gamma_2^2}{\gamma_2^2}\right)(Y \sin\beta_2 + Z \cos\beta_2)$$

$$F_1 = \frac{\beta_2^2}{\gamma_2^2}(Y \sin\beta_2 a + Z \cos\beta_2 a - W \sin\beta_1 a)$$

$$F_2 = \sin\gamma_2 a + \alpha_1 \cos\gamma_2 a$$

$$F_3 = \alpha_2 \cos\gamma_2 a + F_1$$

$$\alpha_5 = \frac{F_2}{\sin\gamma_1 a}$$

$$\alpha_6 = \frac{F_3}{\sin\gamma_1 a}$$

$$F_4 = \alpha_5 \sin\gamma_1 a$$

$F_5 = \alpha_6 \sin\gamma_1 a + W \sin\beta_1 a$

$F_6 = a$

$\delta_{11} = F_4$

$\delta_{12} = 0$

$\delta_{13} = F_6$

$\delta_{14} = -F_5$

$\delta_{21} = \sin\gamma_2 a + \alpha_1 \cos\gamma_2 a$

$\delta_{22} = a + \alpha_3$

$\delta_{23} = 0$

$\delta_{24} = -(\alpha_2 \cos\gamma_2 a + \alpha_4 + Y \sin\beta_2 a + Z \cos\beta_2 a)$

$\delta_{31} = \gamma_2 \cos\gamma_2 a - \gamma_2\alpha_1 \sin\gamma_2 a - \gamma_1\alpha_5 \cos\gamma_1 a$

$\delta_{32} = 1$

$\delta_{33}=-1$

$\delta_{34}=W\beta_1 \cos\beta_1 a - Y\beta_2 \cos\beta_2 a + Z\beta_2 \sin\beta_2 a + \alpha_6\gamma_1 \cos\gamma_1 a + \alpha_2\gamma_2 \sin\gamma_2 a$

APPENDIX D

Variables Used in Case VI

$$\alpha_1=-\tan\gamma_2$$

$$\alpha_2=-\frac{\beta_2^2}{\gamma_2^2\cos\gamma_2}(Y\sin\beta_2+Z\cos\beta_2)$$

$$\alpha_3=-1$$

$$\alpha_4=\left(\frac{\beta_2^2-\gamma_2^2}{\gamma_2^2}\right)(Y\sin\beta_2+Z\cos\beta_2)$$

$$F_1=\frac{\beta_2^2}{\gamma_2^2}(Y\sin\beta_2 a+Z\cos\beta_2 a-W\sin\beta_1 a)$$

$$F_2=\sin\gamma_2 a+\alpha_1\cos\gamma_2 a$$

$$F_3=\alpha_2\cos\gamma_2 a+F_1$$

$$\alpha_5=\frac{F_2}{\sin\gamma_1 a}$$

$$\alpha_6=\frac{F_3}{\sin\gamma_1 a}$$

$$F_4=-\gamma_2^3\cos\gamma_2 a$$

$$F_5 = \gamma_2^3 \sin\gamma_2 a$$

$$F_6 = -Y\beta_2^3 \cos\beta_2 a + Z\beta_2^3 \sin\beta_2 a$$

$$F_7 = \sin\gamma_1 a$$

$$F_8 = W \sin\beta_1 a$$

$$F_9 = -\gamma_1^3 \cos\gamma_1 a$$

$$F_{10} = -W\beta_1^3 \cos\beta_1 a$$

$$F_{11} = \gamma_1^2 F_4 + \gamma_1^2 \alpha_1 F_5 + \gamma_2^2 (k F_7 - F_9) \alpha_5$$

$$F_{12} = \alpha_2 \gamma_1^2 F_5 + \gamma_1^2 F_6 + \gamma_2^2 \alpha_6 (k F_7 - F_9) + \gamma_2^2 (k F_8 - F_{10})$$

$$F_{13} = \gamma_2^2 ka$$

$$\delta_{11} = F_{11}$$

$$\delta_{12} = 0$$

$$\delta_{13} = F_{13}$$

$\delta_{14}=-F_{12}$

$\delta_{21}=\sin\gamma_2 a+\alpha_1 \cos\gamma_2 a-\alpha_5 \sin\gamma_1 a$

$\delta_{22}=a+\alpha_3$

$\delta_{23}=-a$

$\delta_{24}=W \sin\beta_1 a-Y \sin\beta_2 a-Z \cos\beta_2 a+\alpha_6 \sin\gamma_1 a-\alpha_2 \cos\gamma_2 a-\alpha_4$

$\delta_{31}=\gamma_2 \cos\gamma_2 a-\gamma_2\alpha_1 \sin\gamma_2 a-\gamma_1\alpha_5 \cos\gamma_1 a$

$\delta_{32}=1$

$\delta_{33}=-1$

$\delta_{34}=W\beta_1 \cos\beta_1 a-Y\beta_2 \cos\beta_2 a+Z\beta_2 \sin\beta_2 a+\alpha_6\gamma_1 \cos\gamma_1 a+\alpha_2\gamma_2 \sin\gamma_2 a$

APPENDIX E

Variables Used in Case VII

$$\alpha_1 = -\tan\gamma_2$$

$$\alpha_2 = -\frac{\beta_2^2}{\gamma_2^2 \cos\gamma_2}(Y \sin\beta_2 + Z \cos\beta_2)$$

$$F_1 = \frac{\beta_2^2}{\gamma_2^2}(Y \sin\beta_2 a + Z \cos\beta_2 a - W \sin\beta_1 a)$$

$$F_2 = \sin\gamma_2 a + \alpha_1 \cos\gamma_2 a$$

$$F_3 = \alpha_2 \cos\gamma_2 a + F_1$$

$$\alpha_5 = \frac{F_2}{\sin\gamma_1 a}$$

$$\alpha_6 = \frac{F_3}{\sin\gamma_1 a}$$

$$F_4 = -\gamma_2^3 \cos\gamma_2 a$$

$$F_5 = \gamma_2^3 \sin\gamma_2 a$$

$$F_6 = -Y\beta_2^3 \cos\beta_2 a + Z\beta_2^3 \sin\beta_2 a$$

$$F_7 = \sin\gamma_1 a$$

$$F_8 = W \sin\beta_1 a$$

$$F_9 = -\gamma_1^3 \cos\gamma_1 a$$

$$F_{10} = -W\beta_1^3 \cos\beta_1 a$$

$$F_{11} = \gamma_1^2 F_4 + \gamma_1^2 \alpha_1 F_5 + \gamma_2^2 (k_1 F_7 - F_9) \alpha_5$$

$$F_{12} = \alpha_2 \gamma_1^2 F_5 + \gamma_1^2 F_6 + \gamma_2^2 \alpha_6 (k_1 F_7 - F_9) + \gamma_2^2 (k_1 F_8 - F_{10})$$

$$F_{13} = \gamma_2^2 k_1 a$$

$$G_1 = \beta_2^3 (-Y \cos\beta_2 + Z \sin\beta_2) + \beta_2^2 (\widetilde{B}_1 \beta_2 \cos\beta_2 - \widetilde{B}_2 \beta_2 \sin\beta_2 + \widetilde{B}_3)$$
$$+ \gamma_2^2 (Y\beta_2 \cos\beta_2 - Z\beta_2 \sin\beta_2) - \frac{\gamma_2^2}{\gamma_1^2} k_2 (Y \sin\beta_2 + Z \cos\beta_2)$$

$$G_2 = \gamma_2^2 - \frac{\gamma_2^2}{\gamma_1^2} k_2$$

$$G_3 = -\frac{\gamma_2^2}{\gamma_1^2} k_2$$

$$G_4 = -\frac{\gamma_2^2}{\gamma_1^2} k_2(\sin\gamma_2 + \alpha_1 \cos\gamma_2)$$

$$G_5 = -\frac{\gamma_2^2}{\gamma_1^2} k_2\alpha_2 \cos\gamma_2$$

$$G_6 = -\frac{G_4}{G_3}$$

$$G_7 = -\frac{G_2}{G_3}$$

$$G_8 = \frac{1}{G_3}(-G_1 - G_5)$$

$$\delta_{11} = F_{11}$$

$$\delta_{12} = 0$$

$$\delta_{13} = F_{13}$$

$$\delta_{14} = -F_{12}$$

$$\delta_{21} = \sin\gamma_2 a + \alpha_1 \cos\gamma_2 a - \alpha_5 \sin\gamma_1 a + G_6$$

$$\delta_{22} = a + G_7$$

$\delta_{23}=-a$

$\delta_{24}=\alpha_6 \sin\gamma_1 a-\alpha_2 \cos\gamma_2 a-G_8+W \sin\beta_1 a-Y \sin\beta_2 a-Z \cos\beta_2 a$

$\delta_{31}=\gamma_2 \cos\gamma_2 a-\gamma_2\alpha_1 \sin\gamma_2 a-\gamma_1\alpha_5 \cos\gamma_1 a$

$\delta_{32}=1$

$\delta_{33}=-1$

$\delta_{34}=W\beta_1 \cos\beta_1 a-Y\beta_2 \cos\beta_2 a+Z\beta_2 \sin\beta_2 a+\alpha_6\gamma_1 \cos\gamma_1 a+\alpha_2\gamma_2 \sin\gamma_2 a$

VITA

Jae-Guen Yang was born on June 25, 1962, in Seoul, Korea. He graduated from Sung Mun High School in Seoul, Korea, in February, 1981. He entered Yonsei University in Seoul, Korea, in March, 1981. He received his B.S. degree in Architectural Engineering in February, 1985. He continued his education at the same university as a graduate student. He received his M.S. degree in Architectural Engineering, specializing in Structures, in February, 1987.

He began his graduate studies at Virginia Polytechnic Institute and State University in September, 1990. He is receiving an M.S. degree in Civil Engineering in December, 1991. He is going to continue his studies as a Ph.D. student at the same university starting from January, 1992.

LATERAL BRACING FORCES IN COMPRESSED TWO-SPAN COLUMNS WITH INITIAL CURVATURE

by

Jae-Guen Yang

(ABSTRACT)

The main purpose of this study is to find critical loads and full bracing conditions for perfect two-span columns, and to find the reaction forces at the lateral bracing supports and maximum deflections for two-span columns with initial curvature. In each case, the column under consideration may have different bending stiffnesses in each span, and the column is subjected to an axial compressive load. The braces are not assumed to be equally spaced, and may have different spring stiffnesses.

For the perfect columns, it is found that if the internal lateral support is located in the middle of the column , the column can resist a higher applied load than for any other support location. The load resisting capacity of the column depends on the lateral spring stiffnesses. It is also found that an ideal spring stiffness, corresponding to full bracing, only exists under special conditions.

For the imperfect columns, the initial shape is assumed to be the same as the buckling mode of the perfect column, and its size is specified. It is found that there are no reaction forces when there is full bracing. The reaction forces and maximum deflections are proportional to the size of the initial deflection, so their values for initial deflections of the same shape but different size can be determined directly from the results presented here.